



Letter

Measurement of substructure-dependent suppression of large-radius jets with charged particles in Pb + Pb collisions with ATLAS

The ATLAS Collaboration¹

ARTICLE INFO

Editor: Dr. M. Doser

Keywords:

Jet quenching
 Quark-gluon plasma
 Relativistic heavy-ion collisions
 Jets & heavy flavor physics

ABSTRACT

Measurements of jet substructure in Pb + Pb collisions provide key insights into the mechanism of jet quenching in the hot and dense QCD medium created in these collisions. This Letter presents a measurement of the suppression of large-radius jets with a radius parameter of $R = 1.0$ and its dependence on the jet substructure. The measurement uses 1.72 nb^{-1} of Pb + Pb data and 255 pb^{-1} of pp data, both at $\sqrt{s_{\text{NN}}} = 5.02 \text{ TeV}$, recorded with the ATLAS detector at the Large Hadron Collider. Large-radius jets are reconstructed by reclustering $R = 0.2$ calorimetric jets and are measured for transverse momentum above 200 GeV. Jet substructure is evaluated using charged-particle tracks, and the overall level of jet suppression is quantified using the jet nuclear modification factor (R_{AA}). The jet R_{AA} is measured as a function of jet p_{T} , the charged k_i splitting scale ($\sqrt{d_{12}}$), and the angular separation (ΔR_{12}) of two leading sub-jets. The jet R_{AA} gradually decreases with increasing $\sqrt{d_{12}}$, implying significantly stronger suppression of large-radius jets with larger k_i splitting scale. The jet R_{AA} gradually decreases for ΔR_{12} in the range 0.01–0.2 and then remains consistent with a constant for $\Delta R_{12} \gtrsim 0.2$. The observed significant dependence of jet suppression on the jet substructure will provide new insights into its role in the quenching process.

1. Introduction

Collisions of heavy ions at the Relativistic Heavy Ion Collider (RHIC) and the Large Hadron Collider (LHC) [1] allow one to study the interaction between showers of high transverse momentum (p_{T}) partons produced in hard-scattering processes and quark-gluon plasma (QGP) formed as a result of copious liberation of colour charges during the nuclear collisions [2,3]. The parton showers, which can be described within perturbative quantum chromodynamics, give rise to jets of hadrons that can be measured in a detector. The interactions between the parton shower and the QGP can reduce the energies of jets and modify their substructure [4–9]. These jet modifications are referred to as *jet quenching* and are measured with a variety of observables at RHIC and the LHC [10–12]. Developing a quantitative theoretical description of jet quenching is an open problem that requires detailed experimental input.

One of the important mechanisms contributing to the modification of jet substructure is coherent radiation. When the parton shower propagates through the QGP medium, colour coherence makes the medium-induced gluon radiation unable to resolve small-angle splittings of the parton shower. This implies that a part of the parton shower containing small-angle splittings radiates coherently as a single colour charge [13–15]. Consequently, the colour coherence leads to an over-

all smaller energy loss for smaller-angle splittings than for the case of larger-angle splittings that interact incoherently with the QGP [16]. To describe this phenomenon, a parameter quantifying what part of the collimated shower is resolved needs to be introduced. Typically, this parameter is the resolution length L_{res} [17] or, in an approximation of multiple soft scatterings in QGP, the (de)coherence angle θ_c [13,18]. Two partons in the shower separated by a distance or angle smaller than L_{res} or θ_c are not resolved by the medium.

Several recent measurements using various jet substructure observables [12,18] have provided experimental input that may help to quantify the resolution parameter. In particular, these include measurements of splitting functions, groomed jet radius, and jet girth [19–24]; measurements of the number of splittings and the N -subjettiness [23,25]; and double-differential measurements of jet fragmentation [26]. To isolate sub-jets entering the calculation of substructure observables, two strategies are used in these measurements. The first strategy relies on reclustering the constituents of jets [27] and employing a grooming method, such as Soft Drop [28,29]. The second strategy relies on clustering jets with small radii ($R = 0.2$) that satisfy a minimum- p_{T} requirement into a jet with large radius ($R = 1.0$). The latter strategy was used in Ref. [24], where a significantly weaker suppression of reclustered $R = 1.0$ jets composed of single sub-jets was seen in comparison with reclustered $R = 1.0$ jets composed of multiple sub-jets. Reclustered $R = 1.0$ jets are used also in the study presented here and they are called large- R jets in the subsequent text.

A recent theoretical study [30], which analysed the response of the QGP to the passing jet within the Hybrid strong/weak coupling

Contact: atlas.publications@cern.ch.

¹ Authors are listed at the end of this paper.

model [31], demonstrated that large- R jet substructure measurements may be used to directly constrain L_{res} . However, that study also shows that the coarse binning of substructure observables used in Ref. [24], due to the use of calorimetric objects only, does not allow precise quantification of L_{res} . This limitation is a consequence of the fact that two $R = 0.2$ jets are separated by a minimum angular distance of approximately 0.2. To overcome this limitation, objects possessing better angular resolution, namely charged-particle tracks, may be used to study jet substructure. The approach with charged-particle tracks matched to calorimeter energy clusters was previously used in the substructure study in Ref. [22], where grooming was applied to jets with the traditional radius of $R = 0.4$. The measurement presented here uses large- R jets together with charged-particle tracks to study jet substructure over the broad range of angular separation between sub-jets. The new measurement thus connects the high angular resolution of charged-particle tracks with the large phase-space coverage and precision of large- R calorimetric jets. This approach should, therefore, help to quantify the impact of colour coherence on the jet energy loss.

The measurement presented in this Letter uses data collected by the ATLAS experiment in Pb+Pb and pp collisions at a centre-of-mass energy of 5.02 TeV per colliding nucleon pair. The Pb+Pb and pp data samples contain 1.72 nb^{-1} and 255 pb^{-1} of collision data, respectively.

2. Experimental set-up

The ATLAS experiment [32] at the LHC is a multipurpose particle detector with a forward-backward symmetric cylindrical geometry and nearly 4π coverage in solid angle.² It consists of an inner tracking detector surrounded by a thin superconducting solenoid providing a 2 T axial magnetic field, electromagnetic and hadronic calorimeters, and a muon spectrometer.

The inner tracking detector covers the pseudorapidity range $|\eta| < 2.5$. It consists of silicon pixel, silicon microstrip, and transition radiation tracking detectors. The calorimeter system consists of a sampling liquid-argon (LAr) electromagnetic (EM) calorimeter covering $|\eta| < 3.2$, a steel-scintillator sampling hadronic calorimeter covering $|\eta| < 1.7$, LAr hadronic calorimeters covering $1.5 < |\eta| < 3.2$, and two LAr forward calorimeters (FCal) covering $3.1 < |\eta| < 4.9$. The endcap and forward regions are thus instrumented with LAr calorimeters for EM and hadronic energy measurements up to $|\eta| = 4.9$. A zero-degree calorimeter (ZDC) was situated at $|\eta| > 8.3$ during Pb+Pb data-taking. It is composed of alternating layers of quartz rods and tungsten plates, and is mostly sensitive to spectator neutrons from fragmenting nuclei in Pb+Pb collisions.

A two-level trigger system is used to select events [33]. The first-level trigger is implemented in hardware and uses a subset of the detector information to accept events at a rate close to 100 kHz. This is followed by a software-based trigger that reduces the accepted rate of complete events to 1.25 kHz on average depending on the data-taking conditions. A software suite [34] is used in data simulation, in the reconstruction and analysis of real and simulated data, in detector operations, and in the trigger and data acquisition systems of the experiment.

3. Data and Monte Carlo selection

The Pb+Pb and pp data used in these measurements were collected in 2018 and 2017 [35], respectively. Events were selected using a combination of calorimeter-based jet triggers [33,36]. Both the pp and

Pb+Pb events are required to contain at least one primary vertex reconstructed within 150 mm of the nominal interaction point along the beam axis [37]. Only events taken during stable beam conditions and satisfying detector and data-quality requirements, which include normal operation of the calorimeters and inner tracking detectors, are considered. All jets in the analysis are in a kinematic range where the jet trigger is fully efficient. The Pb+Pb data contain only a small fraction of events ($< 0.5\%$) with multiple collisions per bunch crossing, and these are suppressed using the anti-correlation of signals from the ZDC and FCal. The pp data were collected with typically 1.4–4.4 inelastic interactions per bunch crossing. No Pile-up rejection is applied in the analysis of pp data.

The level of overall event activity, or *centrality*, in Pb+Pb collisions is characterized using the total transverse energy in the forward calorimeter, $\Sigma E_{\text{T}}^{\text{FCal}}$. The $\Sigma E_{\text{T}}^{\text{FCal}}$ distribution is divided into percentiles of the total inelastic cross-section for Pb+Pb collisions. Events in different ranges of $\Sigma E_{\text{T}}^{\text{FCal}}$ are associated with an underlying Pb+Pb collision geometry according to a Monte Carlo (MC) Glauber simulation which also allows us to define the nuclear thickness function, $\langle T_{\text{AA}} \rangle$ [38,39]. This measurement uses five centrality intervals corresponding to the following $\Sigma E_{\text{T}}^{\text{FCal}}$ percentiles, ordered from the most central to the most peripheral collisions (highest to lowest $\Sigma E_{\text{T}}^{\text{FCal}}$): 0–10%, 10–20%, 20–40%, 40–60%, and 60–80%.

The performance of the detector and of the analysis procedure for pp collisions is evaluated using 3.2×10^7 MC events. This simulation sample comprises PYTHIA 8.2 [40] dijet events generated at a centre-of-mass energy of $\sqrt{s} = 5.02$ TeV with the A14 set of tuned parameters [41] and the NNPDF2.3LO parton distribution functions (PDFs) [42]. Pileup from additional pp collisions was generated by PYTHIA 8.1 [43], with the same PDFs and the parameter values set to the A3 tune [44], and the distribution of the number of extra collisions was matched to that of data. A separate sample of 3.2×10^7 simulated events was produced to evaluate the performance of the detector and analysis procedure for Pb+Pb collisions. This simulation sample was produced from minimum-bias Pb+Pb data events overlaid with hard-scattering PYTHIA 8 dijet pp events generated at a centre-of-mass energy of $\sqrt{s} = 5.02$ TeV with the same tune and PDFs as used in generating the pp MC sample for pp collisions. This procedure accurately reproduces the impact of the underlying event on track reconstruction and the detector's response to jets. This sample is reweighted on an event-by-event basis to ensure that the $\Sigma E_{\text{T}}^{\text{FCal}}$ distribution is the same as is measured in the data sample. The detector's response in both samples was simulated utilizing GEANT4 [45,46].

4. Jet and track reconstruction

Two types of objects from the event reconstruction enter the analysis: calorimetric jets and charged-particle tracks from the inner detector. Jets are reconstructed using the anti- k_r algorithm [47,48] with a radius parameter of $R = 0.2$. The jet reconstruction procedure follows that used previously in Pb+Pb collisions [49,50], and is summarized here. Calorimeter cells in all calorimeter layers, with their energy at the electromagnetic scale, are grouped into $\Delta\eta \times \Delta\phi = 0.1 \times \pi/32$ logical towers. The towers are used as the input to the initial jet-finding performed using the $R = 0.2$ anti- k_r algorithm. After the initial jet-finding, the contribution from the underlying event (UE) to the energy deposited in the towers is estimated on an event-by-event basis. This is done by averaging over energies deposited in towers at a given η position. During the averaging and subsequent subtraction, the ϕ dependence arising from the global collective flow in Pb+Pb collisions is also taken into account. Information from towers within $\Delta R = 0.4$ of jet candidates is excluded from the estimate of UE energy. The energies in towers inside jets are updated to subtract the estimated UE contribution, and the UE procedure is iterated using a better-defined set of jets to define the exclusion regions. The resulting jet kinematics are corrected using p_T - and η -dependent factors, determined from simulation, to account for the response of the calorimeter to jets [51]. An additional correction for

² ATLAS uses a right-handed coordinate system with its origin at the nominal interaction point (IP) in the centre of the detector and the z -axis along the beam pipe. The x -axis points from the IP to the centre of the LHC ring, and the y -axis points upwards. Polar coordinates (r, ϕ) are used in the transverse plane, ϕ being the azimuthal angle around the z -axis. The pseudorapidity is defined in terms of the polar angle θ as $\eta = -\ln \tan(\theta/2)$ and is equal to the rapidity $y = (1/2) \ln[(E + p_z)/(E - p_z)]$ in the relativistic limit. Angular distance is measured in units of $\Delta R \equiv \sqrt{(\Delta y)^2 + (\Delta\phi)^2}$.

the absolute response in data is based on in situ studies of pp collisions where jets recoil against photons, Z bosons, or jets in other regions of the calorimeter [51]. This calibration is followed by a cross-calibration that relates the jet energy scale (JES) in high-luminosity 13 TeV pp collisions [52], used for in situ studies, to that of jets reconstructed in the 5.02 TeV data using the procedure outlined above. The same jet reconstruction procedure, without the azimuthal modulation of the UE, is also applied to pp collisions. The UE subtraction in pp collisions removes the Pile-up-contribution to the jet.

Charged-particle tracks are reconstructed from hits in the inner detector using the standard ATLAS track reconstruction algorithm with settings optimized for the high hit density in heavy-ion collisions [53]. Only tracks with p_T greater than 4 GeV are used in this analysis. A requirement on the minimum number of hits and maximum number of holes, where a hole is defined as the absence of a hit expected to be on the track trajectory, ensures the high quality of reconstructed tracks. In order to suppress the contribution from secondary particles, requirements are imposed on the distance of closest approach of the track to the primary vertex in the transverse (d_0) and longitudinal ($z_0 \sin(\theta)$) directions. These requirements vary with p_T and η , but they do not exceed 0.3 mm for d_0 and 0.5 mm for $z_0 \sin(\theta)$ at $p_T = 4$ GeV. The track reconstruction efficiency is approximately 80 % and 85 % in Pb + Pb and pp collisions, respectively. The multiplicity of charged-particle tracks with $p_T > 4$ GeV in large- R jets with $200 < p_T < 251$ GeV reaches a value of approximately 7 in pp collisions.

5. Analysis procedure

The reconstruction of large- R jets follows the procedure introduced in Ref. [24]. First, $R = 0.2$ anti- k_t jets are reconstructed in the calorimeter using the method described in Section 4. The $R = 0.2$ jets with $p_T > 35$ GeV and $|\eta| < 3.0$ are then reclustered using the anti- k_t algorithm with radius parameter $R = 1.0$ to form so-called large- R jets. This approach enables measurements over a broad kinematic range, mitigates the impact of the UE, prevents possible biases from the recovery of quenched-jet energy that is transferred outside the $R = 0.2$ sub-jets, and reduces systematic uncertainties [24]. This approach also allows to define sub-jets using the information from the reclustering of $R = 0.2$ jets and to calculate substructure observables of interest. The use of $R = 0.2$ sub-jets, however, suffers from the limitation on the minimum angular separation between the sub-jets, which is close to 0.2. To overcome this limitation, charged particles reconstructed as tracks in the inner detector are used in this measurement to define sub-jets of large- R jets, without changing the kinematics of large- R jets. Details of the sub-jet definition are given in the next paragraph.

First, charged-particle tracks with $p_T > 4$ GeV that satisfy the requirements specified in Section 4 are matched to $R = 1.0$ jets. The track-to-jet matching is done by *ghost-association* [54,55], where tracks are treated as being infinitesimally soft, with $p_T = 1$ eV. The tracks with this replaced p_T are added to the list of inputs together with the $R = 0.2$ jets to be clustered into $R = 1.0$ jets with the anti- k_t algorithm. This allows the matching to proceed, while the infinitesimally low p_T of tracks implies that they do not affect the reconstruction of large- R jets. Tracks with their original kinematics associated with a $R = 1.0$ jet are then reclustered using the k_t clustering algorithm [56] with $R = 2.5$. While the majority of tracks would be clustered with a radius parameter $R = 1.0$, the larger radius parameter is used in the k_t algorithm to cover edge effects and ensure that all associated tracks are clustered into one jet. The reclustering is performed with the Soft Drop grooming condition applied with parameters $z_{\text{cut}} = 0.15$, which optimizes the suppression of the UE contribution, and $\beta = 0$, which guarantees that the grooming has no impact on the angular structure of the jet; applying Soft Drop condition does not invoke a separate running of Cambridge/Aachen algorithm. Approximately 5 % of the jets fail to satisfy the Soft Drop condition and are not considered in the analysis. Furthermore, the ratio of the Σp_T of tracks associated with a jet to the reconstructed p_T of the calorimetric jet

is required to be greater than 0.2 because the absence of charged particles would undermine meaningful substructure evaluation. This requirement also enhances the robustness of the unfolding procedure which is defined later. The same requirement is applied to particle-level jets. The coverage of the inner tracking detector, along with the choice of radius parameter R for track reclustering, limits the pseudorapidity selection requirement for large- R jets to $|\eta| < 1.3$.

The reclustering gives access to the two leading track-based sub-jets of each large- R jet and defines their angular separation, ΔR_{12} , and k_t splitting scale, $\sqrt{d_{12}}$, as

$$\Delta R_{12} = \sqrt{(\Delta y_{12})^2 + (\Delta \phi_{12})^2}, \quad \sqrt{d_{12}} = \min(p_{T1}, p_{T2}) \times \Delta R_{12}.$$

The ΔR_{12} and $\sqrt{d_{12}}$ were used in the previous study [24] and are directly sensitive to the medium resolution and hardness or virtuality of the splitting. Due to the Soft Drop condition with z_{cut} , the phase space of ΔR_{12} and $\sqrt{d_{12}}$ is correlated, as very soft splittings at large angular separation are removed by grooming.

The $R = 0.2$ jets are defined at the particle level in the MC sample before detector simulation by applying the anti- k_t algorithm with $R = 0.2$ to stable particles with a proper lifetime greater than 30 ps but excluding muons and neutrinos, which do not leave significant energy deposits in the calorimeter. The same kinematic requirements, the same reclustering procedure, and the same ghost-association procedure to match particles to jets that are applied to detector-level jets are also applied at the particle level to obtain particle-level jets in simulation.

To quantify the magnitude of quenching effects, the jet nuclear modification factor R_{AA} of large- R jets is evaluated. It is defined as the ratio of per-event jet yields measured in Pb + Pb collisions normalized by $\langle T_{AA} \rangle$ to the jet cross-section measured in pp collisions [57]. The large- R -jet yields in Pb + Pb collisions, cross-sections in pp collisions, and jet R_{AA} are measured differentially in jet p_T , and ΔR_{12} or $\sqrt{d_{12}}$. The measurement is performed for jets with transverse momentum greater than 200 GeV. This ensures that UE fluctuations do not affect the sub-jet reconstruction and kinematics. The binning chosen for the measured distributions provides an optimal balance between statistical precision and resolution effects, and also follows that used in an earlier measurement of large- R jets [24] to allow a direct comparison.

The jet reconstruction performance for large- R jets is evaluated using MC simulations. The average ratio of the reconstructed jet p_T to the corresponding particle-level jet p_T is found to be unity within 3%. The inclusive and differential distributions are corrected for detector effects using the iterative Bayesian unfolding method [58,59] in one and two dimensions, respectively, to reproduce the particle-level distributions. This correction accounts for bin migrations due to the jet energy resolution (JER) and JES, as well as combinatorial sub-jet contributions arising from UE fluctuations and additional hard partonic interactions in Pb + Pb collisions. To better model the data, simulated distributions are reweighted as a function of the reconstruction-level jet p_T , $\sqrt{d_{12}}$, and ΔR_{12} using the reconstruction-level data-to-simulation ratio prior to unfolding. The number of unfolding iterations is chosen to ensure stability of the results while minimizing statistical uncertainty amplification. Four iterations are used for inclusive $R = 0.2$ and $R = 1.0$ jet yields and cross-sections, while six and eight iterations are applied to $\sqrt{d_{12}}$ and ΔR_{12} distributions in the two-dimensional unfolding, respectively. Particle-level jets that do not match a reconstructed jet satisfying the selection criteria are incorporated as an inefficiency correction after unfolding. A correction is also applied to account for the migration in rapidity, i.e. for the presence of jets reconstructed within a selected rapidity region that have associated particle-level jets with rapidity outside of that region, and vice versa.

6. Systematic uncertainties

The following sources of systematic uncertainty are considered: JES, JER, the sensitivity of the unfolding to the prior, and tracking-related

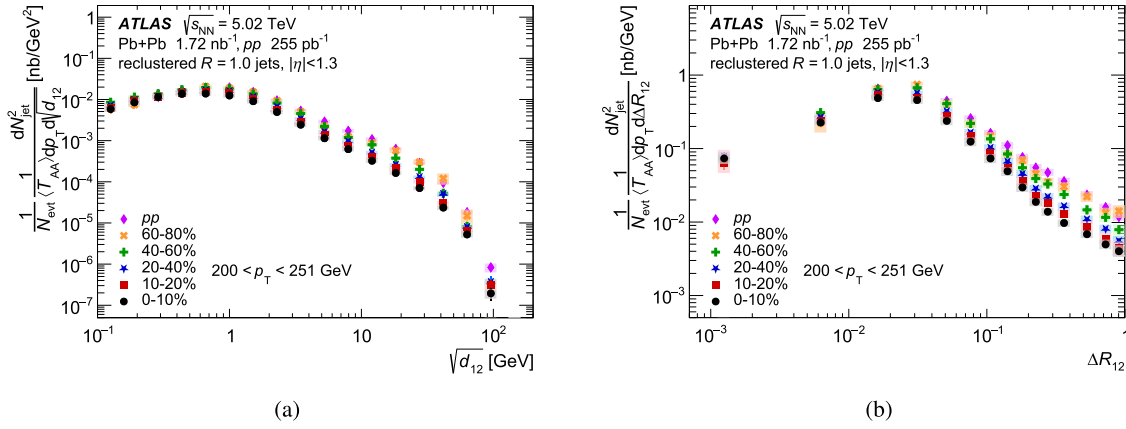


Fig. 1. Measured cross-sections in pp collisions and $\langle T_{AA} \rangle$ -normalized per-event yields in Pb+Pb collisions, evaluated as a function of (a) $\sqrt{d_{12}}$ and (b) ΔR_{12} , for reclustered $R = 1.0$ jets in the p_T interval 200–251 GeV. Normalized yields are shown for five centrality bins of Pb+Pb collisions. The vertical bars on the data points indicate statistical uncertainties, while the shaded boxes indicate systematic uncertainties. The shown systematic uncertainties do not include the uncertainties in the luminosity and $\langle T_{AA} \rangle$ determinations, which are correlated for all the data points and are listed in Section 6.

and overall normalization uncertainties. For each variation accounting for a source of systematic uncertainty, all unfolded distributions, along with their R_{AA} ratios, are re-evaluated. The difference between the varied and nominal distributions is used as an estimate of the uncertainty.

The systematic uncertainties from the JES and JER are evaluated by varying the reconstructed jet energy in simulation. The JES uncertainty is split into three parts: 1) a centrality-independent baseline determined from calorimetric studies [51] plus relative energy-scale differences between heavy-ion and 13 TeV pp jet reconstruction [52]; 2) additional components accounting for the quark/gluon composition of parton showers [49]; and 3) a centrality-dependent component accounting for a different calorimetric response to jets with a modified parton shower due to quenching in Pb+Pb collisions [49,52]. The last component is evaluated by comparing the calorimetric p_T with the summed p_T of charged particles within the jet, and reaches about 1% in central events. The JER uncertainty is assessed by repeating the unfolding with additional Gaussian smearing of the particle-level jet p_T , where the smearing factor is derived from dijet energy-balance studies in 13 TeV pp data [51] and includes additional contributions to account for the different heavy-ion jet reconstruction procedure.

Uncertainties related to track reconstruction and selection arise from several sources. First, the uncertainty due to the detector material description is evaluated by varying the material model in simulation; this can affect the track reconstruction efficiency by approximately 0.5–1.8% in the p_T range used in this analysis [60]. Second, the uncertainty associated with track selection is determined by comparing the results of using the default criteria with those of using different track-quality selections. This leads to variations in the fractions of primary, fake, and secondary tracks and to different tracking efficiencies. Third, the uncertainty due to fake and secondary tracks is estimated as 100% of their contribution determined in MC simulation. Finally, an additional 0.4% uncertainty is assigned to account for the reduced tracking efficiency in regions of high local track density within jet cores [61].

The systematic uncertainty in the unfolding procedure is assessed by constructing response matrices without applying the reweighting used to match the shapes of the charged-particle and jet distributions observed in the data.

Finally, there are uncertainties in the overall normalization of the measured distributions. This includes the uncertainty of 1.0% in the determination of the pp luminosity [62,63] and uncertainties of 0.5%, 0.9%, 1.8%, 3.9%, and 7.1% in the determination of $\langle T_{AA} \rangle$ values [49] for successive centrality intervals from the most central to the most peripheral. The leading systematic uncertainties affecting the yields arise from the JES, at approximately 10%, followed by an approximately 5%

contribution from JER uncertainties. Uncertainties from track reconstruction and unfolding are smaller, typically below 2% or 3%, respectively. The magnitude of these uncertainties shows a mild dependence on both $\sqrt{d_{12}}$ and ΔR_{12} , typically increasing slightly as these variables approach either their highest or lowest values. When evaluating the uncertainty in R_{AA} , the uncertainties common to both pp and Pb+Pb collisions, namely the centrality-independent JES, JER, and tracking uncertainties, are treated as being correlated. Thus, the uncertainty in R_{AA} is typically almost halved relative to uncertainties in the yields.

7. Results

The distributions of $\sqrt{d_{12}}$ for large- R jets in the p_T interval 200–251 GeV measured in pp collisions and five centrality bins of Pb+Pb collisions are shown in Fig. 1(a). All $\sqrt{d_{12}}$ distributions have similar shape, rising at low $\sqrt{d_{12}}$ values, reaching a maximum at $\sqrt{d_{12}} \approx 1$ GeV, and then decreasing. This shape was seen in the previous measurement with large- R jets [24], albeit with the maximum shifted towards larger $\sqrt{d_{12}}$ values as a consequence of using $R = 0.2$ jets above a higher p_T threshold as the input to the reclustering. The distributions of ΔR_{12} for the same kinematic range and event selections as used for the $\sqrt{d_{12}}$ distributions are shown in Fig. 1(b). All the ΔR_{12} distributions feature the same trend: rising, reaching a maximum, and then decreasing with increasing ΔR_{12} . The maximum is reached at $\Delta R_{12} \approx 0.02$, which is consistent with the value measured for the angular separation of the two leading sub-jets, r_g , in groomed $R = 0.4$ jets in the previous measurement [22] which used charged-particle tracks matched to calorimeter energy clusters to investigate the jet substructure.

To quantitatively assess the differences in the suppression of jets characterized by different values of substructure observables, the R_{AA} of large- R jets is evaluated as a function of $\sqrt{d_{12}}$ and ΔR_{12} in bins of the jet p_T and in five centrality intervals. The R_{AA} evaluated as a function of $\sqrt{d_{12}}$ in the jet p_T interval 200–251 GeV is shown in Fig. 2(a). For values of $\sqrt{d_{12}} \gtrsim 0.7$ GeV, one can clearly see that the suppression increases from peripheral to central collisions. The R_{AA} gradually decreases with increasing $\sqrt{d_{12}}$ in the range $0.7 \lesssim \sqrt{d_{12}} \lesssim 20$ GeV in all centrality bins except the one for 60–80% peripheral collisions. In the 0–10% central collisions, the R_{AA} value decreases from approximately 0.8 to 0.2, implying significantly stronger suppression of large- R jets with a larger k_t splitting scale. In the 60–80% peripheral collisions, the distribution's downward trend with increasing $\sqrt{d_{12}}$ is not pronounced, and the R_{AA} fluctuates around a value of approximately 0.8. For $\sqrt{d_{12}} \lesssim 0.7$ GeV, the R_{AA} is greater than 0.8 and it is not possible to discern a significant difference in R_{AA} value between different centrality bins.

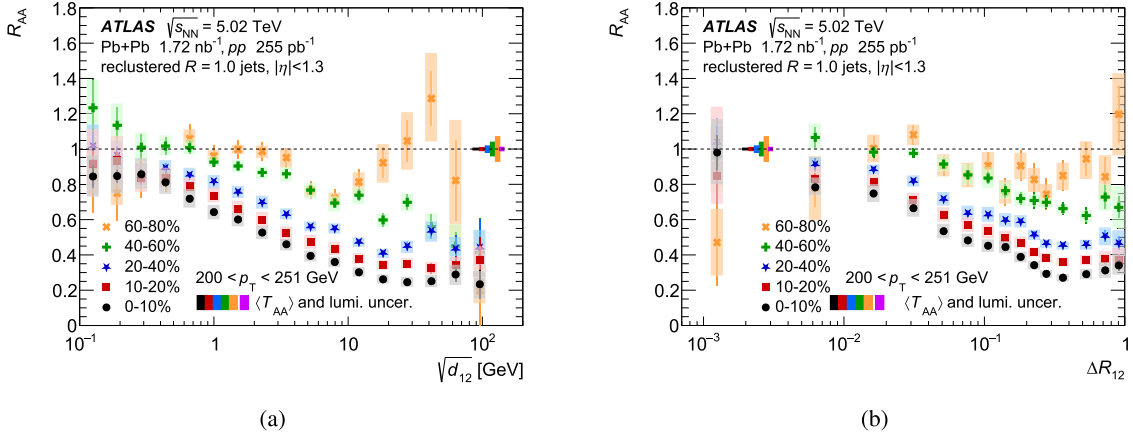


Fig. 2. The R_{AA} of $R = 1.0$ jets evaluated as a function of (a) $\sqrt{d_{12}}$ and (b) ΔR_{12} in five centrality bins and the p_T interval 200–251 GeV. The vertical bars on the data points indicate statistical uncertainties, while the shaded boxes indicate systematic uncertainties. The coloured boxes at $R_{AA} = 1$ represent the fractional per-centrality uncertainty in $\langle T_{AA} \rangle$ and pp luminosity (magenta), which both affect the overall normalization.

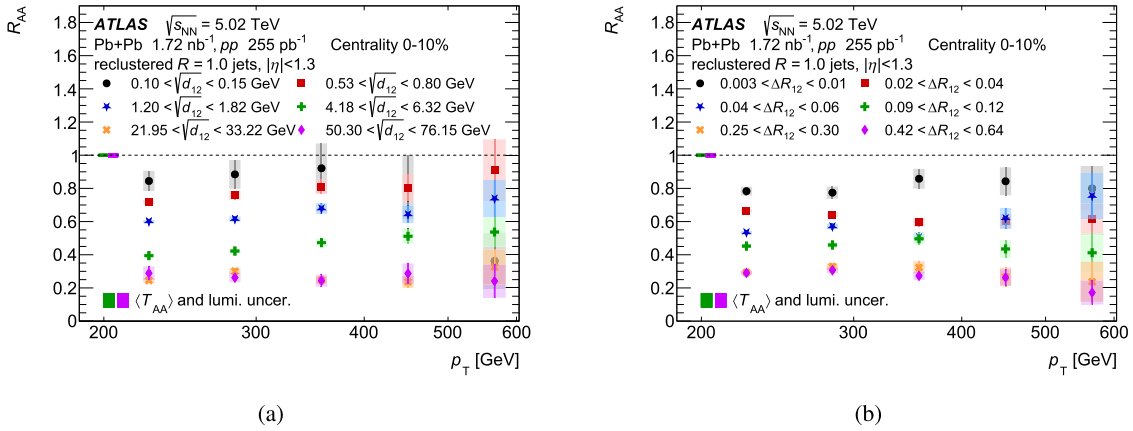


Fig. 3. The R_{AA} of $R = 1.0$ jets in the most central 0–10% collisions evaluated as a function of jet p_T in six intervals of (a) $\sqrt{d_{12}}$ and (b) ΔR_{12} . The vertical bars on the data points indicate statistical uncertainties, while the shaded boxes indicate systematic uncertainties. The coloured boxes at $R_{AA} = 1$ represent the fractional per-centrality uncertainty in $\langle T_{AA} \rangle$ and pp luminosity (magenta), which both affect the overall normalization.

The R_{AA} evaluated as a function of ΔR_{12} for the same kinematic range and centrality bins as in the case of $\sqrt{d_{12}}$ is shown in Fig. 2(b). In the range $0.01 \lesssim \Delta R_{12} \lesssim 0.2$, the R_{AA} decreases in all centrality bins except for 60–80%. For $\Delta R_{12} \lesssim 0.01$, it is not possible to discern a significant difference among centralities because of large uncertainties. For $\Delta R_{12} \gtrsim 0.3$, the R_{AA} values are consistent with being constant within the systematic uncertainties, implying no dependence of the jet suppression on the angular separation of the two sub-jets. This flattening is seen in all centrality selections except for the most peripheral collisions, where the overall jet suppression is small and R_{AA} is more susceptible to statistical fluctuations. The onset of increasing R_{AA} with decreasing values of ΔR_{12} may be partially connected with the suppression difference between narrow and wide jets, but should also be connected with the onset of coherent radiation and should therefore allow one to directly constrain the values of L_{res} and θ_c as discussed, e.g., in Ref. [30]. Similar trends in R_{AA} as a function of $\sqrt{d_{12}}$ and ΔR_{12} are also observed for higher- p_T large- R jets, although with larger statistical uncertainties.

To quantify the jet p_T dependence, the R_{AA} is evaluated in 0–10% central collisions as a function of jet p_T for several $\sqrt{d_{12}}$ and ΔR_{12} bins as shown in Fig. 3(a) and (b), respectively. The substructure-observable bins are selected to quantify the R_{AA} in three distinct regions: the region with low $\sqrt{d_{12}}$ and ΔR_{12} values ($\sqrt{d_{12}} \lesssim 0.5$ GeV, $\Delta R_{12} \lesssim 0.01$); the region with intermediate $\sqrt{d_{12}}$ and ΔR_{12} values ($0.5 \lesssim \sqrt{d_{12}} \lesssim 20$ GeV, $0.01 \lesssim \Delta R_{12} \lesssim 0.3$) where R_{AA} decreases with increasing $\sqrt{d_{12}}$ and ΔR_{12} ; and the region with high $\sqrt{d_{12}}$ and ΔR_{12} values ($\sqrt{d_{12}} \gtrsim 20$ GeV, $\Delta R_{12} \gtrsim 0.3$) where R_{AA} reaches a constant value.

Fig. 3(a) and (b) show that the R_{AA} is independent of jet p_T in the region with low values of the substructure observables. The R_{AA} is also independent of jet p_T in the region with high values of the substructure observables. In the region with intermediate values of the substructure observables, the R_{AA} tends to increase with increasing jet p_T when evaluated in bins of $\sqrt{d_{12}}$. This tendency was confirmed quantitatively by fitting the distribution with a linear function. When evaluated in bins of ΔR_{12} , any such increase is very mild or absent. This quantification of the jet p_T dependence of R_{AA} may further help to constrain the mechanisms responsible for the significant dependence of jet suppression on jet substructure.

The results presented in this Letter are also compared with results from previous studies published in Refs. [22,24]. This comparison is shown in Fig. 4. The R_{AA} evaluated as a function of ΔR_{12} is compared with the R_{AA} of reclustered $R = 1.0$ jets where the $R = 0.2$ sub-jets reconstructed in the calorimeter are used to study the jet substructure [24], and with the R_{AA} of $R = 0.4$ jets where the substructure is quantified using tracks matched to calorimeter energy clusters [22]. The latter measurement evaluated a quantity called r_g , which equates with ΔR_{12} . While the jet definitions and kinematic requirements differ between the measurements, it is still possible to directly compare the reported trends. The values of R_{AA} measured in the flattening region in this Letter are consistent with those reported in Ref. [24]. The new measurement is also consistent with Ref. [22] in the region where R_{AA} decreases with increasing ΔR_{12} (r_g).

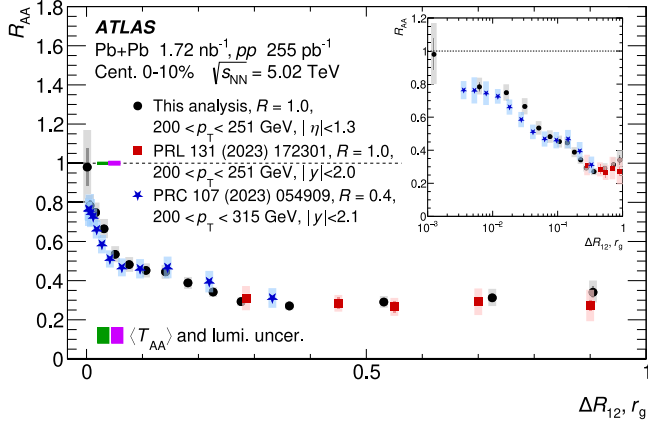


Fig. 4. The R_{AA} of $R = 1.0$ jets evaluated as a function of ΔR_{12} compared with measurements from Ref. [24] ($R = 1.0$ jets with $R = 0.2$ constituents used to define sub-jets) and Ref. [22] ($R = 0.4$ jets with charged-particle tracks matched to calorimeter energy clusters used to define sub-jets). Results are shown in the p_T interval 200–251 GeV for this measurement and the measurement in Ref. [24], and 200–315 GeV for the measurement in Ref. [22]. The inset displays the same distributions using a logarithmic scale, highlighting features at lower ΔR_{12} values. The vertical bars on the data points indicate statistical uncertainties, while the shaded boxes indicate systematic uncertainties. The coloured boxes at $R_{AA} = 1$ represent the fractional uncertainty in $\langle T_{AA} \rangle$ in 0–10% Pb + Pb collisions (green) and pp luminosity (magenta), which both affect the overall normalization. (For interpretation of the references to colour in this figure legend, the reader is referred to the web version of this article.)

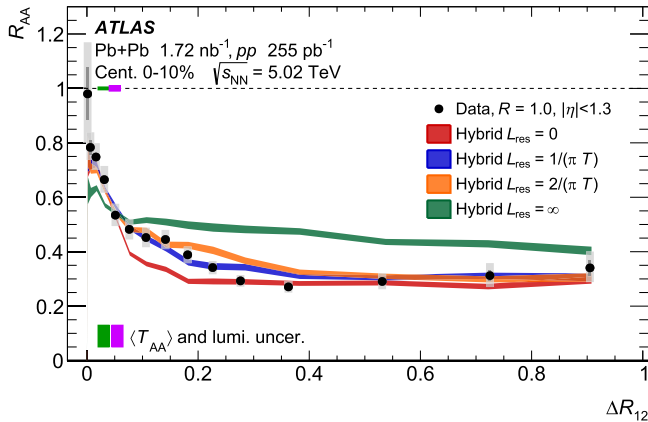


Fig. 5. The R_{AA} of $R = 1.0$ jets as a function of ΔR_{12} is compared to theoretical calculations from the Hybrid model [17,30,31]. Results are shown for 200–251 GeV jets with $|\eta| < 1.3$ in 0–10% Pb + Pb collisions. The theory is displayed as coloured bands corresponding to resolution lengths, $L_{res} = 0$, $1/(\pi T)$, $2/(\pi T)$, and $L_{res} \rightarrow \infty$. The vertical bars on the data points indicate statistical uncertainties, while the shaded boxes indicate systematic uncertainties. The coloured boxes at $R_{AA} = 1$ represent the fractional uncertainties in $\langle T_{AA} \rangle$ (green) and the pp luminosity (magenta), which affect the overall normalisation. (For interpretation of the references to colour in this figure legend, the reader is referred to the web version of this article.)

In the region where R_{AA} decreases, both this measurement and the measurement in Ref. [22] show the possible presence of an inflection point near $\Delta R_{12} \approx 0.1$. Such an inflection point might be connected with the presence of competing mechanisms responsible for the change in R_{AA} . The significance of the presence of an inflection point was determined by fitting a third-order polynomial, and it was found to be 2.8 and 3.6 standard deviations for this measurement and the measurement in Ref. [22], respectively. Evidence for the presence of this inflection point may bring important information for modelling substructure-dependent jet suppression. As a whole, the comparisons presented in

Fig. 4 show that the new measurement allows one to fully quantify the onset of the increase in R_{AA} with decreasing angular separation of the two sub-jets.

A comparison of the data to theoretical calculations from the Hybrid model [17,30,31] is presented in Fig. 5. In the Hybrid model framework, L_{res} represents the earlier discussed resolution length and parametrizes the ability of the medium to resolve the substructure of the jet. The measurement disfavors extreme resolution lengths, namely $L_{res} = 0$ and $L_{res} \rightarrow \infty$, where the exclusion of the latter case was already discussed in [30]. The data exhibit a mild preference for $L_{res} = 1/(\pi T)$ over $L_{res} = 2/(\pi T)$. This comparison demonstrates that the presented measurement has a substantial constraining power on the medium resolution scale and thus should help to quantify the impact of color coherence on measured jet suppression.

8. Conclusion

This Letter presents a measurement of the jet substructure-dependent suppression of large- R jets performed with the ATLAS detector at the LHC using 1.72 nb⁻¹ and 255 pb⁻¹ samples of Pb+Pb and pp collision data, respectively, collected at a centre-of-mass energy of 5.02 TeV per colliding nucleon pair. The jets were reconstructed using the anti- k_t algorithm with $R = 1.0$ by reclustering $R = 0.2$ jets with $p_T > 35$ GeV following the strategy used in a recently published ATLAS analysis. To study the substructure of large- R jets, charged-particle tracks were used, allowing a definition of the two leading sub-jets, their angular separation (ΔR_{12}), and k_t splitting scale ($\sqrt{d_{12}}$). The measurement is corrected to the particle level and presented in bins of jet p_T and collision centrality for jets with $|\eta| < 1.3$ and p_T above 200 GeV.

The jet R_{AA} in the 0–10% central collisions evaluated as a function of $\sqrt{d_{12}}$ gradually decreases with increasing $\sqrt{d_{12}}$, from a value of approximately 0.8 at $\sqrt{d_{12}} \approx 0.7$ GeV to 0.2 at $\sqrt{d_{12}} \approx 20$ GeV, implying significantly stronger suppression of large- R jets with larger k_t splitting scale. The jet R_{AA} evaluated as a function of ΔR_{12} gradually decreases for ΔR_{12} in the range 0.01–0.2 and then remains consistent with a constant value for $\Delta R_{12} \gtrsim 0.2$. A precise evaluation of the onset of ΔR_{12} - and $\sqrt{d_{12}}$ -dependent jet suppression will bring new insights into the role of jet substructure in jet quenching and, in particular, will help to quantitatively constrain the impact of colour coherence on measured jet suppression.

Data availability statement

The public release of data supporting the findings of this article will follow the CERN Open Data Policy [65]. The values of relevant plots and tables associated with this article are stored in HEPData: <https://www.hepdata.net/>.

Declaration of competing interest

The authors declare that they have no known competing financial interests or personal relationships that could have appeared to influence the work reported in this paper.

Acknowledgements

We thank CERN for the very successful operation of the LHC and its injectors, as well as the support staff at CERN and at our institutions worldwide without whom ATLAS could not be operated efficiently. The crucial computing support from all WLCG partners is acknowledged gratefully, in particular from CERN, the ATLAS Tier-1 facilities at TRIUMF/SFU (Canada), NDGF (Denmark, Norway, Sweden), CC-IN2P3 (France), KIT/GridKA (Germany), INFN-CNAF (Italy), NL-T1 (Netherlands), PIC (Spain), RAL (UK) and BNL (USA), the Tier-2 facilities worldwide and large non-WLCG resource providers. Major contributors of computing resources are listed in Ref. [64]. We

gratefully acknowledge the support of ANPCyT, Argentina; YerPhI, Armenia; ARC, Australia; BMWFW and FWF, Austria; ANAS, Azerbaijan; CNPq and FAPESP, Brazil; NSERC, NRC and CFI, Canada; CERN; ANID, Chile; CAS, MOST and NSFC, China; Minciencias, Colombia; MEYS CR, Czech Republic; DNRF and DNSRC, Denmark; IN2P3-CNRS and CEA-DRF/IRFU, France; SRNSFG, Georgia; BMFTR, HGF and MPG, Germany; GSRI, Greece; RGC and Hong Kong SAR, China; ICHEP and Academy of Sciences and Humanities, Israel; INFN, Italy; MEXT and JSPS, Japan; CNRST, Morocco; NWO, Netherlands; RCN, Norway; MNiSW, Poland; FCT, Portugal; MNE/IFA, Romania; MSTDI, Serbia; MSSR, Slovakia; ARIS and MVZI, Slovenia; DSI/NRF, South Africa; MICIU/AEI, Spain; SRC and Wallenberg Foundation, Sweden; SERI, SNSF and Cantons of Bern and Geneva, Switzerland; NSTC, Taipei; TENMAK, Türkiye; STFC/UKRI, United Kingdom; DOE and NSF, United States of America. Individual groups and members have received support from BCKDF, CANARIE, CRC and DRAC, Canada; CERN-CZ, FORTE and PRIMUS, Czech Republic; COST, ERC, ERDF, Horizon 2020, ICSC-NextGenerationEU and Marie Skłodowska-Curie Actions, European Union; Investissements d'Avenir Labex, Investissements d'Avenir IDEX and ANR, France; DFG and AvH Foundation, Germany; Herakleitos, Thales and Aristeia programmes co-financed by EU-ESF and the Greek NSRF, Greece; BSF-NSF and MINERVA, Israel; NCN and NAWA, Poland; La Caixa Banking Foundation, CERCA Programme Generalitat de Catalunya and PROMETEO and GenT Programmes Generalitat Valenciana, Spain; Göran Gustafssons Stiftelse, Sweden; The Royal Society and Leverhulme Trust, United Kingdom. In addition, individual members wish to acknowledge support from Armenia: Yerevan Physics Institute (FAPERJ); CERN: European Organization for Nuclear Research (CERN DOCT); Chile: Agencia Nacional de Investigación y Desarrollo (FONDECYT 1230812, FONDECYT 1240864, Fondecyt 3240661); China: Chinese Ministry of Science and Technology (MOST-2023YFA1605700, MOST-2023YFA1609300), National Natural Science Foundation of China (NSFC - 12175119, NSFC 12275265); Czech Republic: Czech Science Foundation (GACR - 24-11373S), Ministry of Education Youth and Sports (ERC-CZ-LL2327, FORTE CZ.02.01.01/00/22_008/0004632), PRIMUS Research Programme (PRIMUS/21/SCI/017); EU: H2020 European Research Council (ERC - 1011002463); European Union: European Research Council (BARD No. 101116429, ERC - 948254, ERC 101089007), European Regional Development Fund (SMASH COFUND 101081355, SLO ERDF), Horizon 2020 Framework Programme (MUCCA - CHIST-ERA-19-XAI-00), European Union, Future Artificial Intelligence Research (FAIR-NextGenerationEU PE00000013), Horizon 2020 (EuroHPC - EHPC-DEV-2024D11-051), Italian Center for High Performance Computing, Big Data and Quantum Computing (ICSC, NextGenerationEU); France: Agence Nationale de la Recherche (ANR-21-CE31-0022, ANR-22-EDIR-0002); Germany: Baden-Württemberg Stiftung (BW Stiftung-Postdoc Eliteprogramme), Deutsche Forschungsgemeinschaft (DFG - 469666862, DFG - CR 312/5-2); China: Research Grants Council (GRF); Italy: Istituto Nazionale di Fisica Nucleare (ICSC, NextGenerationEU), Ministero dell'Università e della Ricerca (NextGenEU 153D23001490006 M4C2.1.1, NextGenEU 153D23000820006 M4C2.1.1, NextGenEU I53D23001490006 M4C2.1.1, SOE2024.0000023); Japan: Japan Society for the Promotion of Science (JSPS KAKENHI JP22H01227, JSPS KAKENHI JP22H04944, JSPS KAKENHI JP22KK0227, JSPS KAKENHI JP23KK0245, JSPS KAKENHI JP24K23939); Norway: Research Council of Norway (RCN-314472); Poland: Ministry of Science and Higher Education (IDUB AGH, POB8, D4 no 9722), Polish National Science Centre (NCN 2021/42/E/ST2/00350, NCN OPUS 2023/51/B/ST2/02507, NCN OPUS nr 2022/47/B/ST2/03059, NCN UMO-2019/34/E/ST2/00393, UMO-2022/47/O/ST2/00148, UMO-2023/49/B/ST2/04085, UMO-2023/51/B/ST2/00920, UMO-2024/53/N/ST2/00869); Portugal: Foundation for Science and Technology (FCT); Spain: Ministry of Science and Innovation (MCIN & NextGenEU PCI2022-135018-2, MICIN & FEDER PID2021-125273NB, RYC2019-028510-I, RYC2020-030254-I, RYC2021-031273-I, RYC2022-

038164-I); Sweden: Carl Trygger Foundation (Carl Trygger Foundation CTS 22:2312), Swedish Research Council (Swedish Research Council 2023-04654, VR 2021-03651, VR 2022-03845, VR 2022-04683, VR 2023-03403, VR 2024-05451), Knut and Alice Wallenberg Foundation (KAW 2018.0458, KAW 2022.0358, KAW 2023.0366); Switzerland: Swiss National Science Foundation (SNSF - PCEFP2_194658); United Kingdom: Leverhulme Trust (Leverhulme Trust RPG-2020-004), Royal Society (NIF-R1-231091); United States of America: U.S. Department of Energy (ECA DE-AC02-76SF00515), Neubauer Family Foundation.

Appendix

The ATLAS Collaboration

G. Aad¹⁰⁴, E. Aakvaag¹⁷, B. Abbott¹²³, S. Abdelhameed^{119a}, K. Abeling⁵⁵, N.J. Abicht⁴⁹, S.H. Abidi³⁰, M. Aboelela⁴⁵, A. Aboulhorma^{36e}, H. Abramowicz¹⁵⁷, Y. Abulaiti¹²⁰, B.S. Acharya^{69a,69b,n}, A. Ackermann^{63a}, C. Adam Bourdarios⁴, L. Adamczyk^{87a}, S.V. Addepalli¹⁴⁹, M.J. Addison¹⁰³, J. Adelman¹¹⁸, A. Adiguzel^{22c}, T. Adye¹³⁷, A.A. Affolder¹³⁹, Y. Afik⁴⁰, M.N. Agaras¹³, A. Aggarwal¹⁰², C. Agheorghiesei^{28c}, F. Ahmadov^{39,ae}, S. Ahuja⁹⁷, X. Ai^{143b}, G. Aielli^{76a,76b}, A. Aikot¹⁶⁹, M. Ait Tamlihat^{36e}, B. Aitbenkikh^{36a}, M. Akbiyik¹⁰², T.P.A. Åkesson¹⁰⁰, A.V. Akimov¹⁵¹, D. Akiyama¹⁷⁴, N.N. Akolkar²⁵, S. Aktas^{22a}, G.L. Alberghi^{24b}, J. Albert¹⁷¹, P. Albicocco⁵³, G.L. Albouy⁶⁰, S. Alderweireldt⁵², Z.L. Alegria¹²⁴, M. Aleksa³⁷, I.N. Aleksandrov³⁹, C. Alexa^{28b}, T. Alexopoulos¹⁰, F. Alfonsi^{24b}, M. Algren⁵⁶, M. Alhroob¹⁷³, B. Ali¹³⁵, H.M.J. Ali^{93,x}, S. Ali³², S.W. Alibocus⁹⁴, M. Aliev^{34c}, G. Alimonti^{71a}, W. Alkahi⁵⁵, C. Allaire⁶⁶, B.M.M. Allbrooke¹⁵², J.S. Allen¹⁰³, J.F. Allen⁵², P.P. Allport²¹, A. Aloisio^{72a,72b}, F. Alonso⁹², C. Alpigianni¹⁴², Z.M.K. Alsolami⁹³, A. Alvarez Fernandez¹⁰², M. Alves Cardoso⁵⁶, M.G. Alviggi^{72a,72b}, M. Aly¹⁰³, Y. Amaral Coutinho^{83b}, A. Ambler¹⁰⁶, C. Amelung³⁷, M. Ameri¹⁰³, C.G. Ames¹¹¹, T. Amezza¹³⁰, D. Amidei¹⁰⁸, B. Amini⁵⁴, K. Amirie¹⁶¹, A. Amirkhanov³⁹, S.P. Amor Dos Santos^{133a}, K.R. Amos¹⁶⁹, D. Amperiadou¹⁵⁸, S. An⁸⁴, C. Anastopoulos¹⁴⁵, T. Andeen¹¹, J.K. Anders⁹⁴, A.C. Anderson⁵⁹, A. Andreazza^{71a,71b}, S. Angelidakis⁹, A. Angerami⁴², A.V. Anisenkov³⁹, A. Annovi^{74a}, C. Antel³⁷, E. Antipov¹⁵¹, M. Antonelli⁵³, F. Anulli^{75a}, M. Aoki⁸⁴, T. Aoki¹⁵⁹, M.A. Aparo¹⁵², L. Aperio Bella⁴⁸, M. Apicella³¹, C. Appelt¹⁵⁷, A. Apyan²⁷, S.J. Arbiol Val⁸⁸, C. Arcangeletti⁵³, A.T.H. Arce⁵¹, J-F. Arguin¹¹⁰, S. Argyropoulos¹⁵⁸, J.-H. Arling⁴⁸, O. Arnaez⁴, H. Arnold¹⁵¹, G. Artoni^{75a,75b}, H. Asada¹¹³, K. Asai¹²¹, S. Asai¹⁵⁹, S. Asatryan¹⁷⁹, N.A. Asbah³⁷, R.A. Ashby Pickering¹⁷³, A.M. Aslam⁹⁷, K. Assamagan³⁰, R. Astalos^{29a}, K.S.V. Astrand¹⁰⁰, S. Atashi¹⁶⁵, R.J. Atkin^{34a}, H. Atmani^{36f}, P.A. Atlasiddha¹³¹, K. Augsten¹³⁵, A.D. Aurilio¹⁴¹, V.A. Austrup¹⁰³, G. Avolio³⁷, K. Axiotis⁵⁶, G. Azuelos^{110,ai}, A. Azzam¹³, D. Babal^{29b}, H. Bachacou¹³⁸, K. Bachas^{158,r}, A. Bachi³⁵, E. Bachmann⁵⁰, M.J. Backes^{63a}, A. Badea⁴⁰, T.M. Baer¹⁰⁸, P. Bagnaia^{75a,75b}, M. Bahmani¹⁹, D. Bahner⁵⁴, K. Bai¹²⁶, J.T. Baines¹³⁷, L. Baines⁹⁶, O.K. Baker¹⁷⁸, E. Bakos¹⁶, D. Bakshi Gupta⁸, L.E. Balabram Filho^{83b}, V. Balakrishnan¹²³, R. Balasubramanian⁴, E.M. Baldin³⁸, P. Balek^{87a}, E. Ballabene^{24b,24a}, F. Balli¹³⁸, L.M. Baltes^{63a}, W.K. Balunas³³, J. Balz¹⁰², I. Bamwidi^{119b}, E. Banas⁸⁸, M. Bandieramonte¹³², A. Bandopadhyay²⁵, S. Bansal²⁵, L. Barak¹⁵⁷, M. Barakat⁴⁸, E.L. Barberio¹⁰⁷, D. Barberis^{18b}, M. Barbero¹⁰⁴, M.Z. Barel¹¹⁷, T. Barillari¹¹², M-S. Barisits³⁷, T. Barklow¹⁴⁹, P. Baron¹³⁶, D.A. Baron Moreno¹⁰³, A. Baroncelli⁶², A.J. Barr¹²⁹, J.D. Barr⁹⁸, F. Barreiro¹⁰¹, J. Barreiro Guimarães da Costa¹⁴, M.G. Barros Teixeira^{133a}, S. Barsov³⁸, F. Bartels^{63a}, R. Bartoldus¹⁴⁹, A.E. Barton⁹³, P. Bartos^{29a}, A. Basan¹⁰², M. Basella⁴⁹, S. Bashiri⁸⁸, A. Bassalat^{66,b}, M.J. Basso^{162a}, S. Batajau⁴⁵, R. Bate¹⁷⁰, R.L. Bates⁵⁹, S. Batlamous¹⁰¹, M. Battaglia¹³⁹, D. Battulga¹⁹,

M. Baucé^{75a,75b}, M. Bauer⁷⁹, P. Bauer²⁵, L.T. Bayer⁴⁸, L.T. Bazzano Hurrell³¹, J.B. Beacham¹¹², T. Beau¹³⁰, J.Y. Beaucamp⁹², P.H. Beauchemin¹⁶⁴, P. Bechtel²⁵, H.P. Beck^{20,a}, K. Becker¹⁷³, A.J. Beddall⁸², V.A. Bednyakov³⁹, C.P. Bee¹⁵¹, L.J. Beamster¹⁶, M. Begalli^{83d}, M. Biegel³⁰, J.K. Behr⁴⁸, J.F. Beirer³⁷, F. Beisiegel²⁵, M. Belfkir^{119b}, G. Bella¹⁵⁷, L. Bellagamba^{24b}, A. Bellerive³⁵, C.D. Bellgraph⁶⁸, P. Bellos²¹, K. Beloborodov³⁸, D. Benckekroun^{36a}, F. Bendebba^{36a}, Y. Benhammou¹⁵⁷, K.C. Benkendorfer⁶¹, L. Beresford⁴⁸, M. Beretta⁵³, E. Bergeas Kuutmann¹⁶⁷, N. Berger⁴, B. Bergmann¹³⁵, J. Beringer^{18a}, G. Bernardi⁵, C. Bernius¹⁴⁹, F.U. Bernlochner²⁵, F. Bernon³⁷, A. Berrocal Guardia¹³, T. Berry⁹⁷, P. Berta¹³⁶, A. Berthold⁵⁰, A. Berti^{133a}, R. Bertrand¹⁰⁴, S. Bethke¹¹², A. Betti^{75a,75b}, A.J. Bevan⁹⁶, L. Bezio⁵⁶, N.K. Bhalla⁵⁴, S. Bharthuar¹¹², S. Bhatta¹⁵¹, P. Bhattacharai¹⁴⁹, Z.M. Bhatti¹²⁰, K.D. Bhide⁵⁴, V.S. Bhopatkar¹²⁴, R.M. Bianchi¹³², G. Bianco^{24b,24a}, O. Biebel¹¹¹, M. Biglietti^{77a}, C.S. Billingsley⁴⁵, Y. Bimgdi^{36f}, M. Bindi⁵⁵, A. Bingham¹⁷⁷, A. Bingul^{22b}, C. Bini^{75a,75b}, G.A. Bird³³, M. Birman¹⁷⁵, M. Bires¹³⁶, S. Biryukov¹⁵², T. Bisanz⁴⁹, E. Bisceglie^{24b,24a}, J.P. Biswal¹³⁷, D. Biswas¹⁴⁷, I. Bloch⁴⁸, A. Blue⁵⁹, U. Blumenschein⁹⁶, J. Blumenthal¹⁰², V.S. Bobrovnikov³⁹, L. Boccardo^{57b,57a}, M. Boehler⁵⁴, B. Boehm¹⁷², D. Bogavac¹³, A.G. Bogdanchikov³⁸, L.S. Boggia¹³⁰, V. Boisvert⁹⁷, P. Bokan³⁷, T. Bold^{87a}, M. Bomben⁵, M. Bona⁹⁶, M. Boonekamp¹³⁸, A.G. Borbély⁵⁹, I.S. Bordulev³⁸, G. Borisso⁹³, D. Bortoletto¹²⁹, D. Boscherini^{24b}, M. Bosman¹³, K. Bouaouda^{36a}, N. Bouchhar¹⁶⁹, L. Boudet⁴, J. Boudreau¹³², E.V. Bouhova-Thacker⁹³, D. Boumediene⁴¹, R. Bouquet^{57b,57a}, A. Boveia¹²², J. Boyd³⁷, D. Boye³⁰, I.R. Boyko³⁹, L. Bozianu⁵⁶, J. Bracik²¹, N. Brahimi¹, G. Brandt¹⁷⁷, O. Brandt³³, B. Brau¹⁰⁵, J.E. Brau¹²⁶, R. Brenner¹⁷⁵, L. Brenner¹¹⁷, R. Brenner¹⁶⁷, S. Bressler¹⁷⁵, G. Brianti^{78a,78b}, D. Britton⁵⁹, D. Britzger¹¹², I. Brock²⁵, R. Brock¹⁰⁹, G. Brooijmans⁴², A.J. Brooks⁶⁸, E.M. Brooks^{162b}, E. Brost³⁰, L.M. Brown^{171,162a}, L.E. Bruce⁶¹, T.L. Bruckler¹²⁹, P.A. Bruckman de Renstrom⁸⁸, B. Brüers⁴⁸, A. Bruni^{24b}, G. Bruni^{24b}, D. Brunner^{47a,47b}, M. Bruschi^{24b}, N. Brusino^{75a,75b}, T. Buanes¹⁷, Q. Buat¹⁴², D. Buchin¹¹², A.G. Buckley⁵⁹, O. Bulekov⁸², B.A. Bullard¹⁴⁹, S. Burdin⁹⁴, C.D. Burgard⁴⁹, A.M. Burger⁹¹, B. Burghgrave⁸, O. Burlayenko⁵⁴, J. Burlison¹⁶⁸, J.C. Burzynski¹⁴⁸, E.L. Busch⁴², V. Büscher¹⁰², P.J. Bussey⁵⁹, J.M. Butler²⁶, C.M. Buttar⁵⁹, J.M. Butterworth⁹⁸, W. Buttinger¹³⁷, C.J. Buxo Vazquez¹⁰⁹, A.R. Buzykaev³⁹, S. Cabrera Urbán¹⁶⁹, L. Cadamuro⁶⁶, D. Caforio⁵⁸, H. Cai¹³², Y. Cai^{24b,114c,24a}, Y. Cai^{114a}, V.M.M. Cairo³⁷, O. Cakir^{3a}, N. Calace³⁷, P. Calafiura^{18a}, G. Calderini¹³⁰, P. Calfayan³⁵, G. Callea⁵⁹, L.P. Caloba^{83b}, D. Calvet⁴¹, S. Calvet⁴¹, R. Camacho Toro¹³⁰, S. Camarda³⁷, D. Camarero Munoz²⁷, P. Camarri^{76a,76b}, C. Camincher¹⁷¹, M. Campanelli⁹⁸, A. Camplani⁴³, V. Canale^{72a,72b}, A.C. Canbay^{3a}, E. Canonero⁹⁷, J. Cantero¹⁶⁹, Y. Cao¹⁶⁸, F. Capocasa²⁷, M. Capua^{44b,44a}, A. Carbone^{71a,71b}, R. Cardarelli^{76a}, J.C.J. Cardenas⁸, M.P. Cardiff²⁷, G. Carducci^{44b,44a}, T. Carli³⁷, G. Carlino^{72a}, J.I. Carlotta¹³, B.T. Carlson^{132,s}, E.M. Carlson¹⁷¹, J. Carmignani⁹⁴, L. Carminati^{71a,71b}, A. Carnelli⁴, M. Carnesale³⁷, S. Caron¹¹⁶, E. Carquin^{140g}, I.B. Carr¹⁰⁷, S. Carrá^{73a,73b}, G. Carratta^{24b,24a}, A.M. Carroll¹²⁶, M.P. Casado^{72a,72b}, P. Casolaro^{72a,72b}, M. Caspar⁴⁸, F.L. Castillo⁴, L. Castillo Garcia¹³, V. Castillo Gimenez¹⁶⁹, N.F. Castro^{133a,133e}, A. Catinaccio³⁷, J.R. Catmore¹²⁸, T. Cavaliere⁴, V. Cavaliere³⁰, L.J. Caviedes Betancourt^{23b}, E. Celebi⁸², S. Cella³⁷, V. Cepaitis⁵⁶, K. Cerny¹²⁵, A.S. Cerqueira^{83a}, A. Cerri^{74a,74b,al}, L. Cerrito^{76a,76b}, F. Cerutti^{18a}, B. Cervato^{71a,71b}, A. Cervelli^{24b}, G. Cesarini⁵³, S.A. Cetin⁸², P.M. Chabrilat¹³⁰, R. Chakkappal⁶⁶, S. Chakraborty¹⁷³, J. Chan^{18a}, W.Y. Chan¹⁵⁹, J.D. Chapman³³, E. Chapon¹³⁸, B. Chargeishvili^{155b}, D.G. Charlton²¹, C. Chauhan¹³⁶, Y. Che^{114a}, S. Chekanov⁶, S.V. Chekulaev^{162a}, G.A. Chelkov^{39,a}, B. Chen¹⁵⁷, B. Chen¹⁷¹, H. Chen^{114a}, H. Chen³⁰, J. Chen^{144a}, J. Chen¹⁴⁸, M. Chen¹²⁹, S. Chen⁸⁹, S.J. Chen^{114a}, X. Chen^{144a}, X. Chen^{15,ah}, Z. Chen⁶², C.L. Cheng¹⁷⁶, H.C. Cheng^{64a}, S. Cheong¹⁴⁹, A. Cheplakov³⁹, E. Cherepanova¹¹⁷, R. Cherkaoui El Moursli^{36e}, E. Cheu⁷, K. Cheung⁶⁵, L. Chevalier¹³⁸, V. Chiarella⁵³, G. Chiarelli^{74a}, G. Chiodini^{70a}, A.S. Chisholm²¹, A. Chitan^{28b}, M. Chitishvili¹⁶⁹, M.V. Chizhov^{39,t}, K. Choi¹¹, Y. Chou¹⁴², E.Y.S. Chow¹¹⁶, K.L. Chu¹⁷⁵, M.C. Chu^{64a}, X. Chu^{14,114c}, Z. Chubinidze⁵³, J. Chudoba¹³⁴, J.J. Chwastowski⁸⁸, D. Cieri¹¹², K.M. Ciesla^{87a}, V. Cindro⁹⁵, A. Ciocio^{18a}, F. Ciroto^{72a,72b}, Z.H. Citron¹⁷⁵, M. Citterio^{71a}, D.A. Ciubotaru^{28b}, A. Clark⁵⁶, P.J. Clark⁵², N. Clarke Hall⁹⁸, C. Clarry¹⁶¹, S.E. Clawson⁴⁸, C. Clement^{47a,47b}, Y. Coadou¹⁰⁴, M. Cobal^{69a,69c}, A. Coccaro^{57b}, R.F. Coelho Barrue^{133a}, R. Coelho Lopes De Sa¹⁰⁵, S. Coelli^{71a}, L.S. Colangeli¹⁶¹, B. Cole⁴², P. Collado Soto¹⁰¹, J. Collot⁶⁰, R. Coluccia^{70a,70b}, P. Conde Muiño^{133a,133g}, M.P. Connell^{34c}, S.H. Connell^{34c}, E.I. Conroy¹²⁹, M. Contreras Cossio¹¹, F. Conventi^{72a,aj}, A.M. Cooper-Sarkar¹²⁹, L. Corazzina^{75a,75b}, F.A. Corchia^{24b,24a}, A. Cordeiro Oudot Choi¹⁴², L.D. Corpe⁴¹, M. Corradi^{75a,75b}, F. Corriveau^{106,ac}, A. Cortes-Gonzalez¹⁵⁹, M.J. Costa¹⁶⁹, F. Costanza⁴, D. Costanzo¹⁴⁵, B.M. Cote¹²², J. Couthures⁷, G. Cowan⁹⁷, K. Cranmer¹⁷⁶, L. Cremer⁴⁹, D. Cremonini^{24b,24a}, S. Crépé-Renaudin⁶⁰, F. Crescioli¹³⁰, T. Cresta^{73a,73b}, M. Cristinziani¹⁴⁷, M. Cristoforetti^{78a,78b}, V. Croft¹¹⁷, J.E. Crosby¹²⁴, G. Crosetti^{44b,44a}, A. Cueto¹⁰¹, H. Cui⁹⁸, Z. Cui⁷, W.R. Cunningham⁵⁹, F. Curcio¹⁶⁹, J.R. Curran⁵², M.J. Da Cunha Sargedas De Sousa^{57b,57a}, J.V. Da Fonseca Pinto^{83b}, C. Da Via¹⁰³, W. Dabrowski^{87a}, T. Dado³⁷, S. Dahbi¹⁵⁴, T. Dai¹⁰⁸, D. Dal Santo²⁰, C. Dallapiccola¹⁰⁵, M. Dam⁴³, G. D'amen³⁰, V. D'Amico¹¹¹, J. Damp¹⁰², J.R. Dandoy³⁵, D. Dannheim³⁷, G. D'anniballe^{74a,74b}, M. Danner¹⁴⁸, V. Dao¹⁵¹, G. Darbo^{57b}, S.J. Das³⁰, F. Dattola⁴⁸, S. D'Auria^{71a,71b}, A. D'Avanzo^{72a,72b}, T. Davidek¹³⁶, J. Davidson¹⁷³, I. Dawson⁹⁶, K. De⁸, C. De Almeida Rossi¹⁶¹, R. De Asmundis^{72a}, N. De Biase⁴⁸, S. De Castro^{24b,24a}, N. De Groot¹¹⁶, P. de Jong¹¹⁷, H. De la Torre¹¹⁸, A. De Maria^{114a}, A. De Salvo^{75a}, U. De Sanctis^{76a,76b}, F. De Santis^{70a,70b}, A. De Santo¹⁵², J.B. De Vivie De Regie⁶⁰, J. Debevc⁹⁵, D.V. Dedovich³⁹, J. Degens⁹⁴, A.M. Deiana⁴⁵, J. Del Peso¹⁰¹, L. Delagrane¹³⁰, F. Deliot¹³⁸, C.M. Delitzsch⁴⁹, M. Della Pietra^{72a,72b}, D. Della Volpe⁵⁶, A. Dell'Acqua³⁷, L. Dell'Asta^{71a,71b}, M. Delmastro⁴, C.C. Delogu¹⁰², P.A. Delsart⁶⁰, S. Demers¹⁷⁸, M. Demichev³⁹, S.P. Denisov³⁸, H. Denizli^{22a,m}, L. D'Eramo⁴¹, D. Derendarz⁸⁸, F. Derue¹³⁰, P. Dervan^{94,*}, A.M. Desai¹, K. Desch²⁵, F.A. Di Bello^{57b,57a}, A. Di Ciaccio^{76a,76b}, L. Di Ciaccio⁴, A. Di Domenico^{75a,75b}, C. Di Donato^{72a,72b}, A. Di Girolamo³⁷, G. Di Gregorio³⁷, A. Di Luca^{78a,78b}, B. Di Micco^{77a,77b}, R. Di Nardo^{77a,77b}, K.F. Di Petrillo⁴⁰, M. Diamantopoulou³⁵, F.A. Dias¹¹⁷, M.A. Diaz^{140a,140b}, A.R. Didenko³⁹, M. Didenko¹⁶⁹, S.D. Diefenbacher^{18a}, E.B. Diehl¹⁰⁸, S. Diez Cornell⁴⁸, C. Diez Pardos¹⁴⁷, C. Dimitriadis¹⁵⁰, A. Dimitrievska²¹, A. Dimri¹⁵¹, J. Dingfelder²⁵, T. Dingley¹²⁹, I-M. Dinu^{28b}, S.J. Dittmeier^{63b}, F. Dittus³⁷, M. Divisek¹³⁶, B. Dixit⁹⁴, F. Djama¹⁰⁴, T. Djobava^{155b}, C. Doglioni^{103,100}, A. Dohnalova^{29a}, Z. Dolezal¹³⁶, K. Domijan^{87a}, K.M. Dona⁴⁰, M. Donadelli^{83d}, B. Dong¹⁰⁹, J. Donini⁴¹, A. D'Onofrio^{72a,72b}, M. D'Onofrio⁹⁴, J. Dopke¹³⁷, A. Doria^{72a}, N. Dos Santos Fernandes^{133a}, P. Dougan¹⁰³, M.T. Dova⁹², A.T. Doyle⁵⁹, M.A. Draguet¹²⁹, M.P. Drescher⁵⁵, E. Dreyer¹⁷⁵, I. Drivas-koulouris¹⁰, M. Drnevich¹²⁰, M. Drozdova⁵⁶, D. Du⁶², T.A. du Pree¹¹⁷, Z. Duan^{114a}, M. Dubau⁴, F. Dubinin³⁹, M. Dubovsky^{29a}, E. Duchovni¹⁷⁵, G. Duckeck¹¹¹, P.K. Duckett⁹⁸, O.A. Ducu^{28b}, D. Duda⁵², A. Dudarev³⁷, E.R. Duden²⁷, M. D'uffizi¹⁰³, L. Duflot⁶⁶, M. Dührssen³⁷, I. Duminin^{28g}, A.E. Dumitriu^{28b}, M. Dunford^{63a}, S. Dungs⁴⁹, K. Dunne^{47a,47b}, A. Duperrin¹⁰⁴, H. Duran Yildiz^{3a}, M. Düren⁵⁸, A. Durglishvili^{155b}, D. Duvnjak³⁵, G.I. Dyckes^{18a}, M. Dyndal^{87a}, B.S. Dzedzic³⁷

Z.O. Earnshaw¹⁵², G.H. Eberwein¹²⁹, B. Eckerova^{29a}, S. Eggebrecht⁵⁵, E. Egidio Purcino De Souza^{83e}, G. Eigen¹⁷, K. Einsweiler^{18a}, T. Ekelof¹⁶⁷, P.A. Ekman¹⁰⁰, S. El Farkh^{36b}, Y. El Ghazali⁶², H. El Jarrari³⁷, A. El Moussaouy^{36a}, V. Ellajosyula¹⁶⁷, M. Ellert¹⁶⁷, F. Ellinghaus¹⁷⁷, T.A. Elliot⁹⁷, N. Ellis³⁷, J. Elmsheuser³⁰, M. Elsayy^{119a}, M. Elsing³⁷, D. Emeliyanov¹³⁷, Y. Enari⁸⁴, I. Ene^{18a}, S. Epari¹¹⁰, D. Ernani Martins Neto⁸⁸, F. Ernst³⁷, M. Errenst¹⁷⁷, M. Escalier⁶⁶, C. Escobar¹⁶⁹, E. Etzion¹⁵⁷, G. Evans^{133a,133b}, H. Evans⁶⁸, L.S. Evans⁹⁷, A. Ezhilov³⁸, S. Ezzarqtouni^{36a}, F. Fabbri^{24b,24a}, L. Fabbri^{24b,24a}, G. Facini⁹⁸, V. Fadeyev¹³⁹, R.M. Fakhruddinov³⁸, D. Fakkoudis¹⁰², S. Falciano^{75a}, L.F. Falda Ulhoa Coelho^{133a}, F. Fallavollita¹¹², G. Falsetti^{44b,44a}, J. Faltova¹³⁶, C. Fan¹⁶⁸, K.Y. Fan^{64b}, Y. Fan¹⁴, Y. Fang^{14,114c}, M. Fanti^{71a,71b}, M. Faraj^{69a,69b}, Z. Farazpay⁹⁹, A. Farbin⁸, A. Farilla^{77a}, T. Farooque¹⁰⁹, J.N. Farr¹⁷⁸, S.M. Farrington^{137,52}, F. Fassi^{36e}, D. Fassouliotis⁹, L. Fayard⁶⁶, P. Federic¹³⁶, P. Federicova¹³⁴, O.L. Fedin^{38,a}, M. Feickert¹⁷⁶, L. Feligioni¹⁰⁴, D.E. Fellers^{18a}, C. Feng^{143a}, Z. Feng¹¹⁷, M.J. Fenton¹⁶⁵, L. Ferencz⁴⁸, B. Fernandez Barbadillo⁹³, P. Fernandez Martinez⁶⁷, M.J.V. Fernoux¹⁰⁴, J. Ferrando⁹³, A. Ferrari¹⁶⁷, P. Ferrari^{117,116}, R. Ferrari^{73a}, D. Ferrere⁵⁶, C. Ferretti¹⁰⁸, M.P. Fewell¹, D. Fiacco^{75a,75b}, F. Fiedler¹⁰², P. Fiedler¹³⁵, S. Filimonov³⁹, M.S. Filip^{28b,u}, A. Filipčić⁹⁵, E.K. Filmer^{162a}, F. Filthaut¹¹⁶, M.C.N. Fiolhais^{133a,133c}, L. Fiorini¹⁶⁹, W.C. Fisher¹⁰⁹, T. Fitschen¹⁰³, P.M. Fitzhugh¹³⁸, I. Fleck¹⁴⁷, P. Fleischmann¹⁰⁸, T. Flick¹⁷⁷, M. Flores^{34d,ag}, L.R. Flores Castillo^{64a}, L. Flores Sanz De Acedo³⁷, F.M. Follega^{78a,78b}, N. Fomin³³, J.H. Foo¹⁶¹, A. Formica¹³⁸, A.C. Forti¹⁰³, E. Fortin³⁷, A.W. Fortman^{18a}, L. Foster^{18a}, L. Fountas^{9j}, D. Fournier⁶⁶, H. Fox⁹³, P. Francavilla^{74a,74b}, S. Francescato⁶¹, S. Franchellucci⁵⁶, M. Franchini^{24b,24a}, S. Franchino^{63a}, D. Francis³⁷, L. Franco¹¹⁶, V. Franco Lima³⁷, L. Franconi⁴⁸, M. Franklin⁶¹, G. Frattari²⁷, Y.Y. Frid¹⁵⁷, J. Friend⁵⁹, N. Fritzsche³⁷, A. Froch⁵⁶, D. Froidevaux³⁷, J.A. Frost¹²⁹, Y. Fu¹⁰⁹, S. Fuenzalida Garrido^{140g}, M. Fujimoto¹⁰⁴, K.Y. Fung^{64a}, E. Furtado De Simas Filho^{83e}, M. Furukawa¹⁵⁹, J. Fuster¹⁶⁹, A. Gaa⁵⁵, A. Gabrielli^{24b,24a}, A. Gabrielli¹⁶¹, P. Gadow³⁷, G. Gagliardi^{57b,57a}, L.G. Gagnon^{18a}, S. Gaid^{85b}, S. Galantzan¹⁵⁷, J. Gallagher¹, E.J. Gallas¹²⁹, A.L. Gallen¹⁶⁷, B.J. Gallop¹³⁷, K.K. Gan¹²², S. Ganguly¹⁵⁹, Y. Gao⁵², A. Garabaglu¹⁴², F.M. Garay Walls^{140a,140b}, C. Garcia¹⁶⁹, A. Garcia Alonso¹¹⁷, A.G. Garcia Caffaro¹⁷⁸, J.E. Garcia Navarro¹⁶⁹, M.A. Garcia Ruiz^{23b}, M. Garcia-Sciveres^{18a}, G.L. Gardner¹³¹, R.W. Gardner⁴⁰, N. Garelli¹⁶⁴, R.B. Garg¹⁴⁹, J.M. Gargan⁵², C.A. Garner¹⁶¹, C.M. Garvey^{34a}, V.K. Gassmann¹⁶⁴, G. Gaudio^{73a}, V. Gautam¹³, P. Gauzzi^{75a,75b}, J. Gavranovic⁹⁵, I.L. Gavrilenko^{133a}, A. Gavrilyuk³⁸, C. Gay¹⁷⁰, G. Gaycken¹²⁶, E.N. Gazis¹⁰, A. Gekow¹²², C. Gemme^{57b}, M.H. Genest⁶⁰, A.D. Gentry¹¹⁵, S. George⁹⁷, T. Geras⁴⁶, A.A. Gerwin¹²³, P. Gessinger-Befurt³⁷, M.E. Geyik¹⁷⁷, M. Ghani¹⁷³, K. Ghorbanian⁹⁶, A. Ghosal¹⁴⁷, A. Ghosh¹⁶⁵, A. Ghosh⁷, B. Giacobbe^{24b}, S. Giagu^{75a,75b}, T. Giani¹¹⁷, A. Giannini⁶², S.M. Gibson⁹⁷, M. Gignac¹³⁹, D.T. Gil^{87b}, A.K. Gilbert^{87a}, B.J. Gilbert⁴², D. Gillberg³⁵, G. Gilles¹¹⁷, D.M. Gingrich^{2,ai}, M.P. Giordani^{69a,69c}, P.F. Giraud¹³⁸, G. Giugliarelli^{69a,69c}, D. Giugni^{71a}, F. Giuli^{76a,76b}, I. Gkialas^{9,j}, L.K. Gladilin³⁸, C. Glasman¹⁰¹, M. Glazewska²⁰, R.M. Gleason¹⁶⁵, G. Glemza⁴⁸, M. Glisic¹²⁶, I. Gnesi^{44b}, Y. Go³⁰, M. Goblirsch-Kolb³⁷, B. Gocke⁴⁹, D. Godin¹¹⁰, B. Gokturk^{22a}, S. Goldfarb¹⁰⁷, T. Golling⁵⁶, M.G.D. Gololo^{34c}, D. Golubkov³⁸, J.P. Gombas¹⁰⁹, A. Gomes^{133a,133b}, G. Gomes Da Silva¹⁴⁷, A.J. Gomez Delegido¹⁶⁹, R. Gonçalo^{133a}, L. Gonella²¹, A. Gongadze^{155c}, F. Gonnella²¹, J.L. Gonski¹⁴⁹, R.Y. González Andana⁵², S. González de la Hoz¹⁶⁹, M.V. Gonzalez Rodrigues⁴⁸, R. Gonzalez Suarez¹⁶⁷, S. Gonzalez-Sevilla⁵⁶, L. Goossens³⁷, B. Gorini³⁷, E. Gorini^{70a,70b}, A. Gorišek⁹⁵, T.C. Gosart¹³¹, A.T. Goshaw⁵¹, M.I. Gostkin³⁹, S. Goswami¹²⁴, C.A. Gottardo³⁷, S.A. Gotz¹¹¹, M. Goughri^{36b}, A.G. Goussiou¹⁴², N. Govender^{34c}, R.P. Grabarczyk¹²⁹, I. Grabowska-Bold^{87a}, K. Graham³⁵, E. Gramstad¹²⁸, S. Grancagnolo^{70a,70b}, C.M. Grant¹, P.M. Gravila^{28f}, F.G. Gravili^{70a,70b}, H.M. Gray^{18a}, M. Greco¹¹², M.J. Green⁹, C. Greife²⁵, A.S. Grefsrud¹⁷, I.M. Gregor⁴⁸, K.T. Greif¹⁶⁵, P. Grenier¹⁴⁹, S.G. Grewe¹¹², A.A. Grillo¹³⁹, K. Grimm³², S. Grinstein^{13,y}, J.-F. Grivaz⁶⁶, E. Gross¹⁷⁵, J. Grosse-Knetter⁵⁵, L. Guan¹⁰⁸, G. Guerrieri³⁷, R. Guevara¹²⁸, R. Gugel¹⁰², J.A.M. Guhit¹⁰⁸, A. Guida¹⁹, E. Guillon¹⁷³, S. Guindon³⁷, F. Guo^{14,114c}, J. Guo^{144a}, L. Guo⁴⁸, L. Guo^{114b,w}, Y. Guo¹⁰⁸, A. Gupta⁴⁹, R. Gupta¹³², S. Gupta²⁷, S. Gurbuz²⁵, S.S. Gurdasani⁴⁸, G. Gustavino^{75a,75b}, P. Gutierrez¹²³, L.F. Gutierrez Zagazeta¹³¹, M. Gutsche⁵⁰, C. Gutschow⁹⁸, C. Gwenlan¹²⁹, C.B. Gwilliam⁹⁴, E.S. Haaland¹²⁸, A. Haas¹²⁰, M. Habedank⁵⁹, C. Haber^{18a}, H.K. Hadavand⁸, A. Haddad⁴¹, A. Hadeef⁵⁰, A.I. Hagan⁹³, J.J. Hahn¹⁴⁷, E.H. Haines⁹⁸, M. Haleem¹⁷², J. Haley¹²⁴, G.D. Hallewell¹⁰⁴, L. Halser²⁰, K. Hamano¹⁷¹, H. Hamdaoui¹⁶⁷, M. Hamer²⁵, S.E.D. Hammoud⁶⁶, E.J. Hampshire⁹⁷, J. Han^{143a}, L. Han^{114a}, L. Han⁶², S. Han¹⁴, K. Hanagaki⁸⁴, M. Hance¹³⁹, D.A. Hangal⁴², H. Hanif⁴⁸, M.D. Hank¹³¹, J.B. Hansen⁴³, P.H. Hansen⁴³, D. Harada⁵⁶, T. Harenberg¹⁷⁷, S. Harkusha¹⁷⁹, M.L. Harris¹⁰⁵, Y.T. Harris²⁵, J. Harrison¹³, N.M. Harrison¹²², P.F. Harrison¹⁷³, M.L.E. Hart⁹⁸, N.M. Hartman¹¹², N.M. Hartmann¹¹¹, R.Z. Hasan^{97,137}, Y. Hasegawa¹⁴⁶, F. Haslbeck¹²⁹, S. Hassan¹⁷, R. Hauser¹⁰⁹, M. Haviernik¹³⁶, C.M. Hawkes²¹, R.J. Hawkins³⁷, Y. Hayashi¹⁵⁹, D. Hayden¹⁰⁹, C. Hayes¹⁰⁸, R.L. Hayes¹¹⁷, C.P. Hays¹²⁹, J.M. Hays⁹⁶, H.S. Hayward⁹⁴, M. He^{14,114c}, Y. He⁴⁸, Y. He⁹⁸, N.B. Heatley⁹⁶, V. Hedberg¹⁰⁰, C. Heidegger⁵⁴, K.K. Heidegger⁵⁴, J. Heilman³⁵, S. Heim⁴⁸, T. Heim^{18a}, J.G. Heinlein¹³¹, J.J. Heinrich¹²⁶, L. Heinrich¹¹², J. Hejbal¹³⁴, M. Helbig⁵⁰, A. Held¹⁷⁶, S. Hellesund¹⁷, C.M. Helling¹⁷⁰, S. Hellman^{47a,47b}, A.M. Henriques Correia³⁷, H. Herde¹⁰⁰, Y. Hernández Jiménez¹⁵¹, L.M. Herrmann²⁵, T. Herrmann⁵⁰, G. Herten⁵⁴, R. Hertenberger¹¹¹, L. Hervas³⁷, M.E. Hespington¹⁰², N.P. Hessey^{162a}, J. Hessler¹¹², M. Hidaoui^{36b}, N. Hidic¹³⁶, E. Hill¹⁶¹, T.S. Hillersoy¹⁷, S.J. Hillier²¹, J.R. Hinds¹⁰⁹, F. Hinterkeuser²⁵, M. Hirose¹²⁷, S. Hirose¹⁶³, D. Hirschbuehl¹⁷⁷, T.G. Hitchings¹⁰³, B. Hiti⁹⁵, J. Hobbs¹⁵¹, R. Hobincu^{28e}, N. Hod¹⁷⁵, A.M. Hodges¹⁶⁸, M.C. Hodgkinson¹⁴⁵, B.H. Hodgkinson¹²⁹, A. Hoecker³⁷, D.D. Hofer¹⁰⁸, J. Hofer¹⁶⁹, M. Holzbock³⁷, L.B.A.H. Hommels³³, V. Homsak¹²⁹, B.P. Honan¹⁰³, J.J. Hong⁶⁸, T.M. Hong¹³², B.H. Hooberman¹⁶⁸, W.H. Hopkins⁶, M.C. Hoppesch¹⁶⁸, Y. Hori¹¹³, M.E. Horstmann¹¹², S. Hou¹⁵⁴, M.R. Housenga¹⁶⁸, A.S. Howard⁹⁵, J. Howarth⁵⁹, J. Hoya⁶, M. Hrabovsky¹²⁵, T. Hryn'ova⁴, P.J. Hsu⁶⁵, S.-C. Hsu¹⁴², T. Hsu⁶⁶, M. Hu^{18a}, Q. Hu⁶², S. Huang³³, X. Huang^{14,114c}, Y. Huang¹³⁶, Y. Huang^{114b}, Y. Huang¹⁰², Y. Huang¹⁴, Z. Huang⁶⁶, Z. Hubacek¹³⁵, M. Huebner²⁵, F. Huegging²⁵, T.B. Huffman¹²⁹, M. Huftnagel Maranhã De Faria^{83a}, C.A. Hugli⁴⁸, M. Huhtinen³⁷, S.K. Huiberts¹⁷, R. Hulsken¹⁰⁶, C.E. Hultquist^{18a}, D.L. Humphreys¹⁰⁵, N. Huseynov^{12,g}, J. Huston¹⁰⁹, J. Huth⁶¹, R. Hyneman⁷, G. Iacobucci⁵⁶, G. Iakovidis³⁰, L. Iconomidou-Fayard⁶⁶, J.P. Iddon³⁷, P. Iengo^{72a,72b}, R. Iguchi¹⁵⁹, Y. Iiyama¹⁵⁹, T. Iizawa¹⁵⁹, Y. Ikegami⁸⁴, D. Iliadis¹⁵⁸, N. Ilic¹⁶¹, H. Imam^{36a}, G. Inacio Goncalves^{83d}, S.A. Infante Cabanas^{140c}, T. Ingebretsen Carlson^{47a,47b}, J.M. Inglis⁹⁶, G. Introzzi^{73a,73b}, M. Iodice^{77a}, V. Ippolito^{75a,75b}, R.K. Irwin⁹⁴, M. Ishino¹⁵⁹, W. Islam¹⁷⁶, C. Issever¹⁹, S. Istin^{22a,an}, K. Itabashi⁸⁴, H. Ito¹⁷⁴, R. Iuppa^{78a,78b}, A. Ivina¹⁷⁵, V. Izzo^{72a}, P. Jacka¹³⁵, P. Jackson¹, P. Jain⁴⁸, K. Jakobs⁵⁴, T. Jakoubek¹⁷⁵, J. Jamieson⁵⁹, W. Jang¹⁵⁹, S. Jankovych¹³⁶, M. Javurkova¹⁰⁵, P. Jawahar¹⁰³, L. Jeanty¹²⁶, J. Jejelava^{155a,af}, P. Jenni^{54,f}, C.E. Jessiman³⁵, C. Jia^{143a}, H. Jia¹⁷⁰, J. Jia¹⁵¹, X. Jia^{14,114c}, Z. Jia^{114a}, C. Ji⁵², Q. Jiang^{64b}, S. Jiggins⁴⁸, M. Jimenez Ortega¹⁶⁹, J. Jimenez Pena¹³, S. Jin^{114a}, A. Jinaru^{28b}, O. Jinnouchi¹⁴¹, P. Johansson¹⁴⁵, K.A. Johns⁷, J.W. Johnson¹³⁹, F.A. Jolly⁴⁸, D.M. Jones¹⁵², E. Jones⁴⁸, K.S. Jones⁸, P. Jones³³, R.W.L. Jones⁹³,

T.J. Jones⁹⁴, H.L. Joos^{55,37}, R. Joshi¹²², J. Jovicevic¹⁶, X. Ju^{18a}, J.J. Junggeburth³⁷, T. Junkermann^{63a}, A. Juste Rozas^{13,y}, M.K. Jurek⁸⁸, S. Kabana^{140f}, A. Kaczmarska⁸⁸, M. Kado¹¹², H. Kagan¹²², M. Kagan¹⁴⁹, A. Kahn¹³¹, C. Kahra¹⁰², T. Kajji¹⁵⁹, E. Kajomovitz¹⁵⁶, N. Kakati¹⁷⁵, N. Kakoty¹³, I. Kalaitzidou⁵⁴, S. Kandel⁸, N.J. Kang¹³⁹, D. Kar^{34h}, K. Karava¹²⁹, E. Karentzos²⁵, O. Karkout¹¹⁷, S.N. Karpov³⁹, Z.M. Karpova³⁹, V. Kartvelishvili⁹³, A.N. Karyukhin³⁸, E. Kasimi¹⁵⁸, J. Katzy⁴⁸, S. Kaur³⁵, K. Kawade¹⁴⁶, M.P. Kawale¹²³, C. Kawamoto⁸⁹, T. Kawamoto⁶², E.F. Kay³⁷, F.I. Kaya¹⁶⁴, S. Kazakov¹⁰⁹, V.F. Kazanin³⁸, J.M. Keaveney^{34a}, R. Keeler¹⁷¹, G.V. Kehris⁶¹, J.S. Keller³⁵, J.J. Kempster¹⁵², O. Kepka¹³⁴, J. Kerr^{162b}, B.P. Kerridge¹³⁷, B.P. Kerševan⁹⁵, L. Keszezhova^{29a}, R.A. Khan¹³², A. Khanov¹²⁴, A.G. Kharlamov³⁸, T. Kharlamova³⁸, E.E. Khoda¹⁴², M. Kholodenko^{133a}, T.J. Khoo¹⁹, G. Khoriali¹⁷², Y. Khouli^{36a}, J. Khubua^{155b,*}, Y.A.R. Khwaira¹³⁰, B. Kibirige^{34h}, D. Kim⁶, D.W. Kim^{47a,47b}, Y.K. Kim⁴⁰, N. Kimura⁹⁸, M.K. Kingston⁵⁵, A. Kirchoff⁵⁵, C. Kirfel²⁵, F. Kirfel²⁵, J. Kirk¹³⁷, A.E. Kiryunin¹¹², S. Kita¹⁶³, O. Kivernykh²⁵, M. Klassen¹⁶⁴, C. Klein³⁵, L. Klein¹⁷², M.H. Klein⁴⁵, S.B. Klein⁵⁶, U. Klein⁹⁴, A. Klimentov³⁰, T. Klioutchnikova³⁷, P. Kluit¹¹⁷, S. Kluth¹¹², E. Kneringer⁷⁹, T.M. Knight¹⁶¹, A. Knue⁴⁹, M. Kobel⁵⁰, D. Kobylanski¹⁷⁵, S.F. Koch¹²⁹, M. Kocian¹⁴⁹, P. Kodyš¹³⁶, D.M. Koeck¹²⁶, T. Koffas³⁵, O. Kolay⁵⁰, I. Koletsou⁴, T. Komarek⁸⁸, K. Köneke⁵⁵, A.X.Y. Kong¹, T. Kono¹²¹, N. Konstantinidis⁹⁸, P. Kontaxakis⁵⁶, B. Konya¹⁰⁰, R. Kopeliansky⁴², S. Koperny^{87a}, K. Korcyl⁸⁸, K. Kordas^{158,d}, A. Korn⁹⁸, S. Korn⁵⁵, I. Korolkov¹³, N. Korotkova³⁸, B. Kortman¹¹⁷, O. Kortner¹¹², S. Kortner¹¹², W.H. Kostecka¹¹⁸, M. Kostov^{29a}, V.V. Kostyukhin¹⁴⁷, A. Kotskechagia³⁷, A. Kotwali⁵¹, A. Koulouris³⁷, A. Kourkoumeli-Charalampidi^{73a,73b}, C. Kourkoumelis⁹, E. Kourlitis¹¹², O. Kovanda¹²⁶, R. Kowalewski¹⁷¹, W. Kozanecki¹²⁶, A.S. Kozhin³⁸, V.A. Kramarenko³⁸, G. Kramerberger⁹⁵, P. Kramer²⁵, M.W. Krasny¹³⁰, A. Krasznahorkay¹⁰⁵, A.C. Kraus¹¹⁸, J.W. Kraus¹⁷⁷, J.A. Kremer⁴⁸, N.B. Krenkel¹⁴⁷, T. Kresse⁵⁰, L. Kretschmann¹⁷⁷, J. Kretschmar⁹⁴, P. Krieger¹⁶¹, K. Krizka²¹, K. Kroeninger⁴⁹, H. Kroha¹¹², J. Kroll¹³⁴, J. Kroll¹³¹, K.S. Krowpman¹⁰⁹, U. Kruchonak³⁹, H. Krüger²⁵, N. Krumnack⁸¹, M.C. Kruse⁵¹, O. Kuchinskaja³⁹, S. Kuday^{3a}, S. Kuehn³⁷, R. Kuesters⁵⁴, T. Kuhl⁴⁸, V. Kukhtin³⁹, Y. Kulchitsky³⁹, S. Kuleshov^{140d,140b}, J. Kull¹, E.V. Kumar¹¹¹, M. Kumar^{34h}, N. Kumari⁴⁸, P. Kumari^{162b}, A. Kupco¹³⁴, T. Kupfer⁴⁹, A. Kupich³⁸, O. Kuprash⁵⁴, H. Kurashige⁸⁶, L.L. Kurchaninov^{162a}, O. Kurdysh⁴, Y.A. Kurochkin³⁸, A. Kurova³⁸, M. Kuze¹⁴¹, A.K. Kvam¹⁰⁵, J. Kvita¹²⁵, N.G. Kyriacou¹⁰⁸, C. Lacasta¹⁶⁹, F. Lacava^{75a,75b}, H. Lacker¹⁹, D. Lacour¹³⁰, N.N. Lad⁹⁸, E. Ladygin³⁹, A. Lafarge⁴¹, B. Laforge¹³⁰, T. Lagouri¹⁷⁸, F.Z. Lahbabi^{36a}, S. Lai⁵⁵, J.E. Lambert¹⁷¹, S. Lammers⁶⁸, W. Lampl⁷, C. Lampoudis^{158,d}, G. Lamprinouidis¹⁰², A.N. Lancaster¹¹⁸, E. Lançon³⁰, U. Landgraf⁵⁴, M.P.J. Landon⁹⁶, V.S. Lang⁵⁴, O.K.B. Langrekken¹²⁸, A.J. Lankford¹⁶⁵, F. Lanni³⁷, K. Lantzsch²⁵, A. Lanza^{73a}, M. Lanzac Berrocal¹⁶⁹, J.F. Laporte¹³⁸, T. Lari^{71a}, D. Larsen¹⁷, L. Larson¹¹, F. Lasagni Manghi^{24b}, M. Lassnig³⁷, S.D. Lawlor¹⁴⁵, R. Lazaridou¹⁷³, M. Lazzaroni^{71a,71b}, H.D.M. Le¹⁰⁹, E.M. Le Boulicaut¹⁷⁸, L.T. Le Pottier^{18a}, B. Leban^{24b,24a}, F. Ledroit-Guillon⁶⁰, T.F. Lee^{162b}, L.L. Leeuw^{34c}, M. Lefebvre¹⁷¹, C. Leggett^{18a}, G. Lehmann Miotto³⁷, M. Leigh⁵⁶, W.A. Leight¹⁰⁵, W. Leinonen¹¹⁶, A. Leisos^{158,v}, M.A.L. Leite^{83c}, C.E. Leitgeb¹⁹, R. Leitner¹³⁶, K.J.C. Leney⁴⁵, T. Lenz²⁵, S. Leone^{74a}, C. Leonidopoulos⁵², A. Leopold¹⁵⁰, J.H. Lepage Bourbonnais³⁵, R. Les¹⁰⁹, C.G. Lester³³, M. Levchenko³⁸, J. Leveque⁴, L.J. Levinson¹⁷⁵, G. Levri^{24b,24a}, M.P. Lewicki⁸⁸, C. Lewis¹⁴², D.J. Lewis⁴, L. Lewitt¹⁴⁵, A. Li³⁰, B. Li^{143a}, C. Li¹⁰⁸, C-Q. Li¹¹², H. Li^{143a}, H. Li¹⁰³, H. Li¹⁵, H. Li⁶², H. Li^{143a}, J. Li^{144a}, K. Li¹⁴, L. Li^{144a}, R. Li¹⁷⁸, S. Li^{14,114c}, S. Li^{144b,144a}, T. Li⁵, X. Li¹⁰⁶, Z. Li¹⁵⁹, Z. Li^{14,114c}, Z. Li⁶², S. Liang^{14,114c}, Z. Liang¹⁴, M. Liberatore¹³⁸, B. Liberti^{76a}, K. Lie^{64c}, J. Lieber Marin^{83e}, H. Lien⁶⁸, H. Lin¹⁰⁸, S.F. Lin¹⁵¹, L. Linden¹¹¹, R.E. Lindley⁷, J.H. Lindon³⁷, J. Ling⁶¹, E. Lipeles¹³¹, A. Lipniacka¹⁷, A. Lister¹⁷⁰, J.D. Little⁶⁸, B. Liu¹⁴, B.X. Liu^{114b}, D. Liu^{144b,144a}, D. Liu¹³⁹, E.H.L. Liu²¹, J.K.K. Liu¹²⁰, K. Liu^{144b}, K. Liu^{144b,144a}, M. Liu⁶², M.Y. Liu⁶², P. Liu¹⁴, Q. Liu^{144b,142,144a}, X. Liu⁶², X. Liu^{143a}, Y. Liu^{114b,114c}, Y.L. Liu^{143a}, Y.W. Liu⁶², Z. Liu^{66j}, S.L. Lloyd⁹⁶, E.M. Lobodzinska⁴⁸, P. Loch⁷, E. Lodhi¹⁶¹, T. Lohse¹⁹, K. Lohwasser¹⁴⁵, E. Loiaco⁴⁸, J.D. Lomas²¹, J.D. Long⁴², I. Longarini¹⁶⁵, R. Longo¹⁶⁸, A. Lopez Solis¹³, N.A. Lopez-canelas⁷, N. Lorenzo Martinez⁴, A.M. Lory¹¹¹, M. Losada^{119a}, G. Lösckche Centeno¹⁵², X. Lou^{47a,47b}, X. Lou^{14,114c}, A. Lounis⁶⁶, P.A. Love⁹³, M. Lu⁶⁶, S. Lu¹³¹, Y.J. Lu¹⁵⁴, H.J. Lubatti¹⁴², C. Luci^{75a,75b}, F.L. Lucio Alves^{114a}, F. Luehring⁶⁸, B.S. Lunday¹³¹, O. Lundberg¹⁵⁰, J. Lunde³⁷, N.A. Luongo⁶, M.S. Lutz³⁷, A.B. Lux²⁶, D. Lynn³⁰, R. Lysak¹³⁴, V. Lysenko¹³⁵, E. Lytken¹⁰⁰, V. Lyubushkin³⁹, T. Lyubushkina³⁹, M.M. Lyukova¹⁵¹, M. Firdaus M. Soberi⁵², H. Ma³⁰, K. Ma⁶², L.L. Ma^{143a}, W. Ma⁶², Y. Ma¹²⁴, J.C. MacDonald¹⁰², P.C. Machado De Abreu Farias^{83e}, R. Madar⁴¹, T. Madula⁹⁸, J. Maeda⁸⁶, T. Maeno³⁰, P.T. Mafa^{34c,k}, H. Maguire¹⁴⁵, M. Maheshwari³³, V. Maiboroda⁶⁶, A. Maio^{133a,133b,133d}, K. Maj^{87a}, O. Majersky⁴⁸, S. Majewski¹²⁶, R. Makhmanazarov³⁸, N. Makovec⁶⁶, V. Maksimovic¹⁶, B. Malaescu¹³⁰, J. Malamant¹²⁸, Pa. Malecki⁸⁸, V.P. Maleev³⁸, F. Malek^{60,p}, M. Mali⁹⁵, D. Malito⁹⁷, U. Mallik^{80,*}, A. Maloizel⁵, S. Maltezos¹⁰, A. Malvezzi Lopes^{83d}, S. Malyukov³⁹, J. Mamuzic¹³, G. Mancini⁵³, M.N. Mancini²⁷, G. Manco^{73a,73b}, J.P. Mandalia⁹⁶, S.S. Mandarri¹⁵², I. Mandic⁹⁵, L. Manhaes de Andrade Filho^{83a}, I.M. Maniatis¹⁷⁵, J. Manjarres Ramos⁹¹, D.C. Mankad¹⁷⁵, A. Mann¹¹¹, T. Manoussos³⁷, M.N. Mantinan⁴⁰, S. Manzoni³⁷, L. Mao^{144a}, X. Mapekula^{34c}, A. Marantis¹⁵⁸, R.R. Marcelo Gregorio⁹⁶, G. Marchiori⁵, M. Marcisovska¹³⁴, C. Marcon^{71a}, E. Maricic¹⁶, M. Marinescu⁴⁸, S. Marius⁴⁸, M. Marjanovic¹²³, A. Markhoos⁵⁴, M. Markovitch⁶⁶, M.K. Maroun¹⁰⁵, G.T. Marsden¹⁰³, E.J. Marshall⁹³, Z. Marshall^{18a}, S. Marti-Garcia¹⁶⁹, J. Martin⁹⁸, T.A. Martin¹³⁷, V.J. Martin⁵², B. Martin dit Latour¹⁷, L. Martinelli^{75a,75b}, M. Martinez^{13,y}, P. Martinez Agullo¹⁶⁹, V.I. Martinez Outschoorn¹⁰⁵, P. Martinez Suarez¹³, S. Martin-Haugh¹³⁷, G. Martinovicova¹³⁶, V.S. Martoiu^{28b}, A.C. Martyniuk⁹⁸, A. Marzin³⁷, D. Mascione^{78a,78b}, L. Masetti¹⁰², J. Masik¹⁰³, A.L. Maslennikov³⁹, S.L. Mason⁴², P. Massarotti^{72a,72b}, P. Mastrandrea^{74a,74b}, A. Mastroberardino^{44b,44a}, T. Masubuchi¹²⁷, T.T. Mathew¹²⁶, J. Matousek¹³⁶, D.M. Mattern⁴⁹, J. Maurer^{28b}, T. Maurin⁵⁹, A.J. Maury⁶⁶, B. Maček⁹⁵, C. Mavungu Tsava¹⁰⁴, D.A. Maximov³⁸, A.E. May¹⁰³, E. Mayer⁴¹, R. Mazini^{34h}, I. Maznas¹¹⁸, S.M. Mazza¹³⁹, E. Mazzeo³⁷, J.P. Mc Gowan¹⁷¹, S.P. Mc Kee¹⁰⁸, C.A. Mc Lean⁶, C.C. McCracken¹⁷⁰, E.F. McDonald¹⁰⁷, A.E. McDougall¹¹⁷, L.F. Mcelhinney⁹³, J.A. Mcfayden¹⁵², R.P. McGovern¹³¹, R.P. Mckenzie^{34h}, T.C. Mcclachlan⁴⁸, D.J. McLaughlin⁹⁸, S.J. McMahon¹³⁷, C.M. Mcpartland⁹⁴, R.A. McPherson^{171,ac}, S. Mehlhase¹¹¹, A. Mehta⁹⁴, D. Melini¹⁶⁹, B.R. Mellado Garcia^{34h}, A.H. Melo⁵⁵, F. Meloni⁴⁸, A.M. Mendes Jacques Da Costa¹⁰³, L. Meng⁹³, S. Menke¹¹², M. Mentink³⁷, E. Meoni^{44b,44a}, G. Mercado¹¹⁸, S. Merianos¹⁵⁸, C. Merlassino^{69a,69c}, C. Meroni^{71a,71b}, J. Metcalfe⁶, A.S. Mete⁶, E. Meuser¹⁰², C. Meyer⁶⁸, J-P. Meyer¹³⁸, Y. Miao^{114a}, R.P. Middleton¹³⁷, M. Mihovilovic⁶⁶, L. Mijovic⁵², G. Mikenberg¹⁷⁵, M. Mikestikova¹³⁴, M. Mikuz⁹⁵, H. Mildner¹⁰², A. Milic³⁷, D.W. Miller⁴⁰, E.H. Miller¹⁴⁹, L.S. Miller³⁵, A. Milov¹⁷⁵, D.A. Milstead^{47a,47b}, T. Min^{114a}, A.A. Minaenko³⁸, I.A. Minashvili^{155b}, A.I. Mincer¹²⁰, B. Mindur^{87a}, M. Mineev³⁹, Y. Mino⁸⁹, L.M. Mir¹³, M. Miralles Lopez⁵⁹, M. Mironova^{18a}, M. Missio¹¹⁶, A. Mitra¹⁷³, V.A. Mitsou¹⁶⁹, Y. Mitsuori¹¹³, O. Mi¹⁶¹, P.S. Miyagawa⁹⁶, T. Mkrtychan^{63a}, M. Mlinarevic⁹⁸, T. Mlinarevic⁹⁸, M. Mlynarikova³⁷, S. Mobius²⁰, M.H. Mohamed Farook¹¹⁵, S. Mohapatra⁴², S. Mohiuddin¹²⁴,

G. Mokgatitswane^{34h}, L. Moleri¹⁷⁵, U. Molinatti¹²⁹, L.G. Mollier²⁰, B. Mondal¹³⁴, S. Mondal¹³⁵, K. Mönig⁴⁸, E. Monnier¹⁰⁴, L. Monsonis Romero¹⁶⁹, J. Montejo Berlingen¹³, A. Montella^{47a,47b}, M. Montella¹²², F. Montereali^{77a,77b}, F. Monticelli⁹², S. Monzani^{69a,69c}, A. Morancho Tarda⁴³, N. Morange⁶⁶, A.L. Moreira De Carvalho⁴⁸, M. Moreno Llácer¹⁶⁹, C. Moreno Martinez⁵⁶, J.M. Moreno Perez^{23b}, P. Morettini^{57b}, S. Morgenstern³⁷, M. Morii⁶¹, M. Morinaga¹⁵⁹, M. Moritsu⁹⁰, F. Morodei^{75a,75b}, P. Moschovakos³⁷, B. Moser⁵⁴, M. Mosidze^{155b}, T. Moskalets⁴⁵, P. Moskvitina¹¹⁶, J. Moss³², P. Moszkowicz^{87a}, A. Moussa^{36d}, Y. Moyal¹⁷⁵, H. Moyano Gomez¹³, E.J.W. Moyses¹⁰⁵, O. Mtintsilana^{34h}, S. Muanza¹⁰⁴, M. Mucha²⁵, J. Mueller¹³², R. Müller³⁷, G.A. Mullier¹⁶⁷, A.J. Mullin³³, J.J. Mullin⁵¹, A.C. Mullins⁴⁵, A.E. Mulski⁶¹, D.P. Mungo¹⁶¹, D. Munoz Perez¹⁶⁹, F.J. Munoz Sanchez¹⁰³, W.J. Murray^{173,137}, M. Muškinja⁹⁵, C. Mwewa⁴⁸, A.G. Myagkov^{38a}, A.J. Myers⁸, G. Myers¹⁰⁸, M. Myska¹³⁵, B.P. Nachman^{18a}, K. Nagai¹²⁹, K. Nagano⁸⁴, R. Nagasaka¹⁵⁹, J.L. Nagle^{30,ak}, E. Nagy¹⁰⁴, A.M. Nairz³⁷, Y. Nakahama⁸⁴, K. Nakamura⁸⁴, K. Nakkalil⁵, A. Nandi^{63b}, H. Nanjo¹²⁷, E.A. Narayanan⁴⁵, Y. Narukawa¹⁵⁹, I. Naryshkin³⁸, L. Nasella^{71a,71b}, S. Nasri^{119b}, C. Nass²⁵, G. Navarro^{23a}, J. Navarro-Gonzalez¹⁶⁹, A. Nayaz¹⁹, P.Y. Nechaeva³⁸, S. Nechaeva^{24b,24c}, F. Nechansky¹³⁴, L. Nedjc¹²⁹, T.J. Neep²¹, A. Negri^{73a,73b}, M. Negrini^{24b}, C. Nellist¹¹⁷, C. Nelson¹⁰⁶, K. Nelson¹⁰⁸, S. Nemecek¹³⁴, M. Nessi^{37,h}, M.S. Neubauer¹⁶⁸, J. Newell⁹⁴, P.R. Newman²¹, Y.W.Y. Ng¹⁶⁸, B. Ngair^{119a}, H.D.N. Nguyen¹¹⁰, J.D. Nichols¹²³, R.B. Nickerson¹²⁹, R. Nicolaidou¹³⁸, J. Nielsen¹³⁹, M. Niemeyer⁵⁵, J. Niermann³⁷, N. Nikiforou³⁷, V. Nikolaenko^{38a}, I. Nikolic-Audit¹³⁰, P. Nilsson³⁰, I. Ninca⁴⁸, G. Ninio¹⁵⁷, A. Nisati^{75a}, R. Nisius¹¹², N. Nitika^{69a,69c}, J.-E. Nitschke⁵⁰, E.K. Nkadimeng^{34b}, T. Nobe¹⁵⁹, T. Nommensen¹⁵³, M.B. Norfolk¹⁴⁵, B.J. Norman³⁵, M. Noury^{36a}, J. Novak⁹⁵, T. Novak⁹⁵, R. Novotny¹³⁵, L. Nozka¹²⁵, K. Ntekas¹⁶⁵, N.M.J. Nunes De Moura Junior^{83b}, J. Ocariz¹³⁰, A. Ochi⁸⁶, I. Ochoa^{133a}, S. Oerdek^{48,z}, J.T. Offermann⁴⁰, A. Ogrodnik¹³⁶, A. Oh¹⁰³, C.C. Ohm¹⁵⁰, H. Oide⁸⁴, M.L. Ojeda³⁷, Y. Okumura¹⁵⁹, L.F. Oleiro Seabra^{133a}, I. Oleksiyuk⁵⁶, G. Oliveira Correa¹³, D. Oliveira Damazio³⁰, J.L. Oliver¹⁶⁵, R. Omar⁶⁸, Ö.O. Öncel⁵⁴, A.P. O'Neill²⁰, A. Onofre^{133a,133e}, P.U.E. Onyisi¹¹, M.J. Oreglia⁴⁰, D. Orestano^{77a,77b}, R. Orlandini^{77a,77b}, R.S. Orr¹⁶¹, L.M. Osojnak¹³¹, Y. Osumi¹¹³, G. Otero y Garzon³¹, H. Otono⁹⁰, M. Ouchrif^{36d}, F. Ould-Saada¹²⁸, T. Ovsiannikova¹⁴², M. Owen⁵⁹, R.E. Owen¹³⁷, V.E. Ozcan^{22a}, F. Ozturk⁸⁸, N. Ozturk⁸, S. Ozturk⁸², H.A. Pacey¹²⁹, K. Pachal^{162a}, A. Pacheco Pages¹³, C. Padilla Aranda¹³, G. Padovano^{75a,75b}, S. Pagan Griso^{18a}, G. Palacino⁶⁸, A. Palazzo^{70a,70b}, J. Pampel²⁵, J. Pan¹⁷⁸, T. Pan^{64a}, D.K. Panchal¹¹, C.E. Pandini⁶⁰, J.G. Panduro Vazquez¹³⁷, H.D. Pandya¹, H. Pang¹³⁸, P. Pani⁴⁸, G. Panizzo^{69a,69c}, L. Panwar¹³⁰, L. Paolozzi⁵⁶, S. Parajuli¹⁶⁸, A. Paramonov⁶, C. Paraskevopoulos⁵³, D. Paredes Hernandez^{64b}, A. Pareti^{73a,73b}, K.R. Park⁴², T.H. Park¹¹², F. Parodi^{57b,57a}, J.A. Parsons⁴², U. Parzefall⁵⁴, B. Pascual Dias⁴¹, L. Pascual Dominguez¹⁰¹, E. Pasqualucci^{75a}, S. Passaggio^{57b}, F. Pastore⁹⁷, P. Patel⁸⁸, U.M. Patel⁵¹, J.R. Pater¹⁰³, T. Pauly³⁷, F. Pauwels¹³⁶, C.I. Pazos¹⁶⁴, M. Pedersen¹²⁸, R. Pedro^{133a}, S.V. Peleganchuk³⁸, O. Penc¹³⁴, E.A. Pender⁵², S. Peng¹⁵, G.D. Penn¹⁷⁸, K.E. Pensi¹¹¹, M. Penzin³⁸, B.S. Peralva^{83d}, A.P. Pereira Peixoto¹⁴², L. Pereira Sanchez¹⁴⁹, D.V. Perpelitsa^{30,ak}, G. Perera¹⁰⁵, E. Perez Codina³⁷, M. Perganti¹⁰, H. Pernegger³⁷, S. Perrella^{75a,75b}, O. Perrin⁴¹, K. Peters⁴⁸, R.F.Y. Peters¹⁰³, B.A. Petersen³⁷, T.C. Petersen⁴³, E. Petit¹⁰⁴, V. Petousis¹³⁵, A.R. Petri^{71a,71b}, C. Petridou^{158,d}, T. Petru¹³⁶, A. Petrukhin¹⁴⁷, M. Pettee^{18a}, A. Petukhov⁸², K. Petukhova³⁷, E. Pezoa^{140g}, L. Pezzotti^{24b,24a}, G. Pezzullo¹⁷⁸, L. Pfaffenbichler³⁷, A.J. Pflieger³⁷, T.M. Pham¹⁷⁶, T. Pham¹⁰⁷, P.W. Phillips¹³⁷, G. Piacquadio¹⁵¹, E. Pianori^{18a}, F. Piazza¹²⁶, R. Piegaia³¹, D. Pietreanu^{28b}, A.D. Pilkington¹⁰³, M. Pinamonti^{69a,69c}, J.L. Pinfeld², B.C. Pinheiro Pereira^{133a}, J. Pinol Bel¹³, A.E. Pinto Pinoargote¹³⁰, L. Pintucci^{69a,69c}, K.M. Piper¹⁵², A. Pirttikoski⁵⁶, D.A. Pizzi³⁵, L. Pizzimento^{64b}, A. Plebani³³, M.-A. Pleier³⁰, V. Pleskot¹³⁶, E. Plotnikova³⁹, G. Poddar⁹⁶, R. Poettgen¹⁰⁰, L. Poggioli¹³⁰, S. Polacek¹³⁶, G. Polesello^{73a}, A. Poley¹⁴⁸, A. Polini^{24b}, C.S. Pollard¹⁷³, Z.B. Pollock¹²², E. Pompa Pacchi¹²³, N.I. Pond⁹⁸, D. Ponomarenko⁶⁸, L. Pontecorvo³⁷, S. Popa^{28a}, G.A. Popeneciu^{28d}, A. Poreba³⁷, D.M. Portillo Quintero^{162a}, S. Pospisil¹³⁵, M.A. Postill¹⁴⁵, P. Postolache^{28c}, K. Potamianos¹⁷³, P.A. Potepa^{87a}, I.N. Potrap³⁹, C.J. Potter³³, H. Potti¹⁵³, J. Poveda¹⁶⁹, M.E. Pozo Astigarraga³⁷, R. Pozzi³⁷, A. Prades Ibanez^{76a,76b}, J. Pretel¹⁷¹, D. Price¹⁰³, M. Primavera^{70a}, L. Primomo^{69a,69c}, M.A. Principe Martin¹⁰¹, R. Privara¹²⁵, T. Procter^{87b}, M.L. Proffitt¹⁴², N. Proklova¹³¹, K. Prokofiev^{64c}, G. Proto¹¹², J. Proudfoot⁶, M. Przybycien^{87a}, W.W. Przygoda^{87b}, A. Psallidas⁴⁶, J.E. Puddefoot¹⁴⁵, D. Pudza⁵³, D. Pyatizbytantseva¹¹⁶, J. Qian¹⁰⁸, R. Qian¹⁰⁹, D. Qichen¹⁰³, Y. Qin¹³, T. Qiu⁵², A. Quid⁵⁵, M. Queitsch-Maitland¹⁰³, G. Quetant⁵⁶, R.P. Quinn¹⁷⁰, G. Rabanal Bolanos⁶¹, D. Rafanoharana¹¹², F. Raffaelli^{76a,76b}, F. Ragusa^{71a,71b}, J.L. Rainbolt⁴⁰, J.A. Raine⁵⁶, S. Rajagopalan³⁰, E. Ramakoti³⁹, L. Rambelli^{57b,57a}, I.A. Ramirez-Berend³⁵, K. Ran^{48,114c}, D.S. Rankin¹³¹, N.P. Rapheeha^{34h}, H. Rasheed^{28b}, D.F. Rassloff^{63a}, A. Rastogi^{18a}, S. Rave¹⁰², S. Ravera^{57b,57a}, B. Ravina³⁷, I. Ravinovich¹⁷⁵, M. Raymond³⁷, A.L. Read¹²⁸, N.P. Readioff¹⁴⁵, D.M. Rebuffi^{73a,73b}, A.S. Reed¹¹², K. Reeves²⁷, J.A. Reidelsturz¹⁷⁷, D. Reikher¹²⁶, A. Rej⁴⁹, C. Rembser³⁷, H. Ren⁶², M. Renda^{28b}, F. Renner⁴⁸, A.G. Rennie⁵⁹, A.L. Rescia⁴⁸, S. Resconi^{71a}, M. Ressegotti^{57b,57a}, S. Rettie³⁷, W.F. Rettie³⁵, M.M. Revering³³, E. Reynolds^{18a}, O.L. Rezanova³⁹, P. Reznicek¹³⁶, H. Riani^{36d}, N. Riberic⁵¹, E. Ricci^{78a,78b}, R. Richter¹¹², S. Richter^{47a,47b}, E. Richter-Was^{87b}, M. Ridel¹³⁰, S. Ridouani^{36d}, P. Rieck¹²⁰, P. Riedler³⁷, E.M. Riefel^{47a,47b}, J.O. Rieger¹¹⁷, M. Rijssenbeek¹⁵¹, M. Rimoldi³⁷, L. Rinaldi^{24b,24a}, P. Rinke^{167,55}, G. Ripellino¹⁶⁷, I. Riu¹³, J.C. Rivera Vergara¹⁷¹, F. Rizatdinova¹²⁴, E. Rizvi⁹⁶, B.R. Roberts^{18a}, S.S. Roberts¹³⁹, D. Robinson³³, M. Robles Manzano¹⁰², A. Robson⁵⁹, A. Rocchi^{76a,76b}, C. Roda^{74a,74b}, S. Rodriguez Bosca³⁷, Y. Rodriguez Garcia^{23a}, A.M. Rodriguez Vera¹¹⁸, S. Roe³⁷, J.T. Roemer³⁷, O. Röhne¹²⁸, R.A. Rojas³⁷, C.P.A. Roland¹³⁰, A. Romaniouk⁷⁹, E. Romano^{73a,73b}, M. Romano^{24b}, A.C. Romero Hernandez¹⁶⁸, N. Rompotis⁹⁴, L. Roos¹³⁰, S. Rosati^{75a}, B.J. Rosser⁴⁰, E. Rossi¹²⁹, E. Rossi^{72a,72b}, L.P. Rossi⁶¹, L. Rossini⁵⁴, R. Rosten¹²², M. Rotaru^{28b}, B. Rottler⁵⁴, D. Rousseau⁶⁶, D. Rouso⁴⁸, S. Roy-Garand¹⁶¹, A. Rozanov¹⁰⁴, Z.M.A. Rozario⁵⁹, Y. Rozen¹⁵⁶, A. Rubio Jimenez¹⁶⁹, V.H. Ruelas Rivera¹⁹, T.A. Ruggeri¹, A. Ruggiero¹²⁹, A. Ruiz-Martinez¹⁶⁹, A. Rummeler³⁷, Z. Rurikova⁵⁴, N.A. Rusakovich³⁹, H.L. Russell¹⁷¹, G. Russo^{75a,75b}, J.P. Rutherford⁷, S. Rutherford Colmenares³³, M. Rybar¹³⁶, P. Rybczynski^{87a}, A. Ryzhov⁴⁵, J.A. Sabater Iglesias⁵⁶, H.F.-W. Sadrozinski¹³⁹, F. Safai Tehrani^{75a}, S. Saha¹, M. Sahinsoy⁸², B. Sahoo¹⁷⁵, A. Saibel¹⁶⁹, B.T. Saifuddin¹²³, M. Saimpert¹³⁸, G.T. Saito^{83c}, M. Saito¹⁵⁹, T. Saito¹⁵⁹, A. Sala^{71a,71b}, A. Salnikov¹⁴⁹, J. Salt¹⁶⁹, A. Salvador Salas¹⁵⁷, F. Salvatore¹⁵², A. Salzburger³⁷, D. Sammel⁵⁴, E. Sampson⁹³, D. Sampsonidis^{158,d}, D. Sampsonidou¹²⁶, J. Sánchez¹⁶⁹, V. Sanchez Sebastian¹⁶⁹, H. Sandaker¹²⁸, C.O. Sander⁴⁸, J.A. Sandesara¹⁷⁶, M. Sandhoff¹⁷⁷, C. Sandoval^{23b}, L. Sanfilippo^{63a}, D.P.C. Sankey¹³⁷, T. Sano⁸⁹, A. Sansoni⁵³, M. Santana Queiroz^{18b}, L. Santi³⁷, C. Santoni⁴¹, H. Santos^{133a,133b}, A. Santra¹⁷⁵, E. Sanzani^{24b,24c}, K.A. Saoucha^{85b}, J.G. Saraiva^{133a,133d}, J. Sardain⁷, O. Sasaki⁸⁴, K. Sato¹⁶³, C. Sauer³⁷, E. Sauvan⁴, P. Savard^{161,ai}, R. Sawada¹⁵⁹, C. Sawyer¹³⁷, L. Sawyer⁹⁹, C. Sbarra^{24b}, A. Sbrizzi^{24b,24a}, T. Scanlon⁹⁸, J. Schaarschmidt¹⁴², U. Schäfer¹⁰², A.C. Schaffer^{66,45}, D. Schaile¹¹¹, R.D. Schamberger¹⁵¹, C. Scharf¹⁹, M.M. Schefer²⁰,

V.A. Schegelsky³⁸, D. Scheirich¹³⁶, M. Schernau^{140f}, C. Scheulen⁵⁶, C. Schiavi^{57b,57a}, M. Schioppa^{44b,44a}, B. Schlag¹⁴⁹, S. Schlenker³⁷, J. Schmeing¹⁷⁷, E. Schmidt¹¹², M.A. Schmidt¹⁷⁷, K. Schmieden¹⁰², C. Schmitt¹⁰², N. Schmitt¹⁰², S. Schmitt⁴⁸, N.A. Schneider¹¹¹, L. Schoeffel¹³⁸, A. Schoening^{63b}, P.G. Scholer³⁵, E. Schopf¹⁴⁷, M. Schott²⁵, S. Schramm⁵⁶, T. Schroer⁵⁶, H.-C. Schultz-Coulon^{63a}, M. Schumacher⁵⁴, B.A. Schumm¹³⁹, Ph. Schune¹³⁸, H.R. Schwartz¹³⁹, A. Schwartzman¹⁴⁹, T.A. Schwarz¹⁰⁸, Ph. Schwemling¹³⁸, R. Schwienhorst¹⁰⁹, F.G. Sciaccia²⁰, A. Sciandra³⁰, G. Sciolla²⁷, F. Scuri^{74a}, C.D. Sebastiani³⁷, K. Sedlaczek¹¹⁸, S.C. Seidel¹¹⁵, A. Seiden¹³⁹, B.D. Seidlitz⁴², C. Seitz⁴⁸, J.M. Seixas^{83b}, G. Sekhniaidze^{72a}, L. Selem⁶⁰, N. Semprini-Cesari^{24b,24a}, A. Semushin¹⁷⁹, D. Sengupta⁵⁶, V. Senthilkumar¹⁶⁹, L. Serin⁶⁶, M. Sessa^{72a,72b}, H. Severini¹²³, F. Sforza^{57b,57a}, A. Sfyra⁵⁶, Q. Sha¹⁴, E. Shabalina⁵⁵, H. Shaddix¹¹⁸, A.H. Shah³³, R. Shaheen¹⁵⁰, J.D. Shahinian¹³¹, M. Shamim³⁷, L.Y. Shan¹⁴, M. Shapiro^{18a}, A. Sharma³⁷, A.S. Sharma¹⁷⁰, P. Sharma³⁰, P.B. Shatalov³⁸, K. Shaw¹⁵², S.M. Shaw¹⁰³, Q. Shen¹⁴, D.J. Sheppard¹⁴⁸, P. Sherwood⁹⁸, L. Shi⁹⁸, X. Shi¹⁴, S. Shimizu⁸⁴, C.O. Shimm¹⁷⁸, I.P.J. Shipsey^{129,*}, S. Shirabe⁹⁰, M. Shiyakova^{39,aa}, M.J. Shochet⁴⁰, D.R. Shope¹²⁸, B. Shrestha¹²³, S. Shrestha^{122,am}, I. Shreyber³⁹, M.J. Shroff¹⁷¹, P. Sicho¹³⁴, A.M. Sickles¹⁶⁸, E. Sideras Haddad^{34h,166}, A.C. Sidley¹¹⁷, A. Sidoti^{24b}, F. Siegert⁵⁰, Dj. Sijacki¹⁶, F. Sili⁹², J.M. Silva⁵², I. Silva Ferreira^{83b}, M.V. Silva Oliveira³⁰, S.B. Silverstein^{47a}, S. Simion⁶⁶, R. Simonello³⁷, E.L. Simpson¹⁰³, H. Simpson¹⁵², L.R. Simpson⁶, S. Simsek⁸², S. Sindhu⁵⁵, P. Sinervo¹⁶¹, S.N. Singh²⁷, S. Singh³⁰, S. Sinha⁴⁸, S. Sinha¹⁰³, M. Sioli^{24b,24a}, K. Sioulas⁹, I. Siral³⁷, E. Sitnikova⁴⁸, J. Sjölin^{47a,47b}, A. Skaf³⁵, E. Skorda²¹, P. Skubic¹²³, M. Slawinska⁸⁸, I. Slazyk¹⁷, I. Sliuser¹²⁸, V. Smakhtin¹⁷⁵, B.H. Smart¹³⁷, S.Yu. Smirnov^{140b}, Y. Smirnov⁸², L.N. Smirnova^{38,a}, O. Smirnova¹⁰⁰, A.C. Smith⁴², D.R. Smith¹⁶⁵, J.L. Smith¹⁰³, M.B. Smith³⁵, R. Smith¹⁴⁹, H. Smitmans¹⁰², M. Smizanska⁹³, K. Smolek¹³⁵, P. Smolyanskiy¹³⁵, A.A. Snesev³⁹, H.L. Snoek¹¹⁷, S. Snyder³⁰, R. Sobie^{171,ac}, A. Soffer¹⁵⁷, C.A. Solans Sanchez³⁷, E.Yu. Soldatov³⁹, U. Soldevila¹⁶⁹, A.A. Solodkov^{34k}, S. Solomon²⁷, A. Soloshenko³⁹, K. Solovieva⁵⁴, O.V. Solovyanov⁴¹, P. Sommer⁵⁰, A. Sonay¹³, A. Sopczak¹³⁵, A.L. Sapiro⁵², F. Sopkova^{29b}, J.D. Sorenson¹¹⁵, I.R. Sotarriva Alvarez¹⁴¹, V. Sotilingam^{63a}, O.J. Soto Sandoval^{140c,140b}, S. Sottocornola⁶⁸, R. Soualah^{85a}, Z. Soumami^{36e}, D. South⁴⁸, N. Soybelman¹⁷⁵, S. Spagnolo^{70a,70b}, M. Spalla¹¹², D. Sperlich⁵⁴, B. Spisso^{72a,72b}, D.P. Spiteri⁵⁹, L. Splendori¹⁰⁴, M. Spousta¹³⁶, E.J. Staats³⁵, R. Stamen^{63a}, E. Stanecka⁸⁸, W. Stanek-Maslouska⁴⁸, M.V. Stange⁵⁰, B. Stanislaus^{18a}, M.M. Stanitzki⁴⁸, B. Stap⁴⁸, E.A. Starchenko³⁸, G.H. Stark¹³⁹, J. Stark⁹¹, P. Staroba¹³⁴, P. Starovoitov^{85b}, R. Staszewski⁸⁸, G. Stavropoulos⁴⁶, A. Stefi³⁷, P. Steinberg³⁰, B. Stelzer^{148,162a}, H.J. Stelzer¹³², O. Stelzer^{162a}, H. Stenzel³⁸, T.J. Stevenson¹⁵², G.A. Stewart³⁷, J.R. Stewart¹²⁴, M.C. Stockton³⁷, G. Stoica^{28b}, M. Stolarski^{133a}, S. Stonjek¹¹², A. Straessner⁵⁰, J. Strandberg¹⁵⁰, S. Strandberg^{47a,47b}, M. Stratmann¹⁷⁷, M. Strauss¹²³, T. Streblner¹⁰⁴, P. Strizeneck^{29b}, R. Ströhmer¹⁷², D.M. Strom¹²⁶, R. Stroynowski⁴⁵, A. Strubig^{47a,47b}, S.A. Stucci³⁰, B. Stugu¹⁷, J. Stupak¹²³, N.A. Styles⁴⁸, D. Su¹⁴⁹, S. Su⁶², X. Su⁶², D. Suchy^{29a}, K. Sugizaki¹³¹, V.V. Sulim³⁸, M.J. Sullivan⁹⁴, D.M.S. Sultan¹²⁹, L. Sultanaliev³⁸, S. Sultansoy^{3b}, S. Sun¹⁷⁶, W. Sun¹⁴, O. Sunneborn Gudnadottir¹⁶⁷, N. Sur¹⁰⁰, M.R. Sutton¹⁵², H. Suzuki¹⁶³, M. Svatos¹³⁴, P.N. Swallow³³, M. Swiatlowski^{162a}, T. Swirski¹⁷², A. Swoboda³⁷, I. Sykora^{29a}, M. Sykora¹³⁶, T. Sykora¹³⁶, D. Ta¹⁰², K. Tackmann^{48,z}, A. Taffard¹⁶⁵, R. Tahirout^{162a}, Y. Takubo⁸⁴, M. Talby¹⁰⁴, A.A. Talyshev³⁸, K.C. Tam^{64b}, N.M. Tamir¹⁵⁷, A. Tanaka¹⁵⁹, J. Tanaka¹⁵⁹, R. Tanaka⁶⁶, M. Tanasini¹⁵¹, Z. Tao¹⁷⁰, S. Tapia Araya^{140g}, S. Tapprogge¹⁰², A. Tarek Abouelfadl Mohamed¹⁰⁹, S. Tarem¹⁵⁶, K. Tariq¹⁴, G. Tarna³⁷, G.F. Tartarelli^{71a}, M.J. Tartarin⁹¹, P. Tas¹³⁶, M. Tasevsky¹³⁴, E. Tassi^{44b,44a}, A.C. Tate¹⁶⁸, G. Tateno¹⁵⁹, Y. Tayalati^{36e,ab}, G.N. Taylor¹⁰⁷, W. Taylor^{162b}, A.S. Tegetmeier⁹¹, P. Teixeira-Dias⁹⁷, J.J. Teoh¹⁶¹, K. Terashi¹⁵⁹, J. Terron¹⁰¹, S. Terzo¹³, M. Testa⁵³, R.J. Teuscher^{161,ac}, A. Thaler⁷⁹, O. Theiner⁵⁶, T. Theveneaux-Pelzer¹⁰⁴, D.W. Thomas⁹⁷, J.P. Thomas²¹, E.A. Thompson^{18a}, P.D. Thompson²¹, E. Thomson¹³¹, R.E. Thornberry⁴⁵, C. Tian⁶², Y. Tian⁵⁶, V. Tikhomirov⁸², Yu.A. Tikhonov³⁹, S. Timoshenko³⁸, D. Timoshyn¹³⁶, E.X.L. Ting¹, P. Tipton¹⁷⁸, A. Tishelman-Charny³⁰, K. Todome¹⁴¹, S. Todorova-Nova¹³⁶, L. Toffolin^{69a,69c}, M. Togawa⁸⁴, J. Tojo⁹⁰, S. Tokár^{29a}, O. Toldaiev⁶⁸, G. Tolkachev¹⁰⁴, M. Tomoto^{84,113}, L. Tompkins^{149,o}, E. Torrence¹²⁶, H. Torres⁹¹, E. Torró Pastor¹⁶⁹, M. Toscani³¹, C. Toscirì⁴⁰, M. Tost¹¹, D.R. Tovey¹⁴⁵, T. Trefzger¹⁷², P.M. Tricarico¹³, A. Tricoli³⁰, I.M. Trigger^{162a}, S. Trincacz-Duvold¹³⁰, D.A. Trischuk²⁷, A. Tropina³⁹, L. Truong^{34c}, M. Trzebinski⁸⁸, A. Trzupek⁸⁸, F. Tsai¹⁵¹, M. Tsai¹⁰⁸, A. Tsiamis¹⁵⁸, P.V. Tsiarehka³⁹, S. Tsigaridas^{162a}, A. Tsigotis^{158,v}, V. Tsiskaridze^{155a}, E.G. Tskhadadze^{155a}, M. Tsopoulou¹⁵⁸, Y. Tsujikawa⁸⁹, I.I. Tsukerman³⁸, V. Tsulaia^{18a}, S. Tsuno⁸⁴, K. Tsurii¹²¹, D. Tsybychev¹⁵¹, Y. Tu^{64b}, A. Tudorache^{28b}, V. Tudorache^{28b}, S.B. Tuncay¹²⁹, S. Turchikhin^{57b,57a}, I. Turk Cakir^{3a}, R. Turra^{71a}, T. Turtuvshin^{39,ad}, P.M. Tuts⁴², S. Tzamarias^{158,d}, E. Tzovara¹⁰², Y. Uematsu⁸⁴, F. Ukegawa¹⁶³, P.A. Ulloa Poblete^{140c,140b}, E.N. Umaka³⁰, G. Unal³⁷, A. Undrus³⁰, G. Unel¹⁶⁵, J. Urban^{29b}, P. Urrejola^{140a}, G. Usai⁸, R. Ushioda¹⁶⁰, M. Usman¹¹⁰, F. Ustuner⁵², Z. Uysal⁸², V. Vacek¹³⁵, B. Vachon¹⁰⁶, T. Vafeiadis³⁷, A. Vaitkus⁹⁸, C. Valderanis¹¹¹, E. Valdes Santurio^{47a,47b}, M. Valente³⁷, S. Valentinetti^{24b,24a}, A. Valero¹⁶⁹, E. Valiente Moreno¹⁶⁹, A. Vallier⁹¹, J.A. Valls Ferrer¹⁶⁹, D.R. Van Arman¹¹⁷, T.R. Van Daalen¹⁴², A. Van Der Graaf⁴⁹, H.Z. Van Der Schyf^{34h}, P. Van Gemmen⁶, M. Van Rijnbach³⁷, S. Van Stroud⁹⁸, I. Van Vulpen¹¹⁷, P. Vana¹³⁶, M. Vanadia^{76a,76b}, U.M. Vande Voorde¹⁵⁰, W. Vandelli³⁷, E.R. Vandewall¹²⁴, D. Vannicola¹⁵⁷, L. Vannoli⁵³, R. Vari^{75a}, M. Varma¹⁷⁸, E.W. Varnes⁷, C. Varni¹¹⁸, D. Varouchas⁶⁶, L. Varriale¹⁶⁹, K.E. Varvell¹⁵³, M.E. Vasilic^{28b}, L. Vaslin⁸⁴, M.D. Vassilev¹⁴⁹, A. Vasyukov³⁹, L.M. Vaughan¹²⁴, R. Vavricka¹³⁶, T. Vazquez Schroeder¹³, J. Veatch³², V. Vecchio¹⁰³, M.J. Veen¹⁰⁵, I. Veliscek³⁰, E. Velkovska⁹⁵, L.M. Veloce¹⁶¹, F. Veloso^{133a,133c}, S. Veneziano^{75a}, A. Ventura^{70a,70b}, A. Verbitskiy¹¹², M. Verducci^{74a,74b}, C. Vergis⁹⁶, M. Verissimo De Araujo^{83b}, W. Verkerke¹¹⁷, J.C. Vermeulen¹¹⁷, C. Vernieri¹⁴⁹, M. Vessella¹⁶⁵, M.C. Vetterli^{148,ai}, A. Vgenopoulos¹⁰², N. Viaux Maira^{140g}, T. Vickey¹⁴⁵, O.E. Vickey Boeriu¹⁴⁵, G.H.A. Viehhauser¹²⁹, L. Viganò^{63b}, M. Vigi¹¹², M. Villa^{24b,24a}, M. Villaplana Perez¹⁶⁹, E.M. Villhauer⁴⁰, E. Vilucchi⁵³, M. Vincent¹⁶⁹, M.G. Vincker³⁵, A. Visibile¹¹⁷, C. Vittori³⁷, I. Vivarelli^{24b,24a}, E. Voevodina¹¹², F. Vogel¹¹¹, J.C. Voigt⁵⁰, P. Vokac¹³⁵, Yu. Volkotrub^{87b}, E. Von Toerne²⁵, B. Vormwald³⁷, K. Vorobev⁵¹, M. Vos¹⁶⁹, K. Voss¹⁴⁷, M. Vozak³⁷, L. Vozdecky¹²³, N. Vranjes¹⁶, M. Vranjes Milosavljevic¹⁶, M. Vreeswijk¹¹⁷, N.K. Vu^{144b,144a}, R. Vuillermet³⁷, O. Vujanovic¹⁰², I. Vukotic⁴⁰, I.K. Vyas³⁵, J.F. Wack³³, S. Wada¹⁶³, C. Wagner¹⁴⁹, J.M. Wagner^{18a}, W. Wagner¹⁷⁷, S. Wahdan¹⁷⁷, H. Wahlberg⁹², C.H. Waits¹²³, J. Walder¹³⁷, R. Walker¹¹¹, K. Walkingshaw Pass⁵⁹, W. Walkowiak¹⁴⁷, A. Wall¹³¹, E.J. Wallin¹⁰⁰, T. Wamorkar^{18a}, A. Wang⁶², A.Z. Wang¹³⁹, C. Wang¹⁰², C. Wang¹¹, H. Wang^{18a}, J. Wang^{64c}, P. Wang¹⁰³, P. Wang⁹⁸, R. Wang⁶¹, R. Wang⁶, S.M. Wang¹⁵⁴, S. Wang¹⁴, T. Wang⁶², T. Wang⁶², W.T. Wang⁸⁰, W. Wang¹⁴, X. Wang¹⁶⁸, X. Wang^{144a}, X. Wang⁴⁸, Y. Wang^{114a}, Y. Wang⁶², Z. Wang¹⁰⁸, Z. Wang^{144b}, Z. Wang¹⁰⁸, C. Wangetayaraj⁸⁴, A. Warburton¹⁰⁶, A.L. Warnerbring¹⁴⁷, N. Warrack⁵⁹, S. Waterhouse⁹⁷, A.T. Watson²¹, H. Watson⁵², M.F. Watson²¹, E. Watton⁵⁹, G. Watts¹⁴², B.M. Waugh⁹⁸,

J.M. Webb⁵⁴, C. Weber³⁰, H.A. Weber¹⁹, M.S. Weber²⁰, S.M. Weber^{63a}, C. Wei⁶², Y. Wei⁵⁴, A.R. Weidberg¹²⁹, E.J. Weik¹²⁰, J. Weingarten⁴⁹, C. Weiser⁵⁴, C.J. Wells⁴⁸, T. Wenaus³⁰, B. Wendland⁴⁹, T. Wengler³⁷, N.S. Wenke¹¹², N. Vermes²⁵, M. Wessels^{63a}, A.M. Wharton⁹³, A.S. White⁶¹, A. White⁸, M.J. White¹, D. Whiteson¹⁶⁵, L. Wickremasinghe¹²⁷, W. Wiedenmann¹⁷⁶, M. Wieler¹³⁷, R. Wierda¹⁵⁰, C. Wiglesworth⁴³, H.G. Wilkens³⁷, J.J.H. Wilkinson³³, D.M. Williams⁴², H.H. Williams¹³¹, S. Williams³³, S. Willcoq¹⁰⁵, B.J. Wilson¹⁰³, D.J. Wilson¹⁰³, P.J. Windischhofer⁴⁰, F.I. Winkel³¹, F. Winklmeier¹²⁶, B.T. Winter⁵⁴, M. Wittgen¹⁴⁹, M. Wobisch⁹⁹, T. Wojtkowski⁶⁰, Z. Wolfs¹¹⁷, J. Wollrath³⁷, M.W. Wolter⁸⁸, H. Wolters^{133a,133c}, M.C. Wong¹³⁹, E.L. Woodward⁴², S.D. Worm⁴⁸, B.K. Wosiek⁸⁸, K.W. Woźniak⁸⁸, S. Wozniowski⁵⁵, K. Wraight⁵⁹, C. Wu¹⁶¹, C. Wu²¹, J. Wu¹⁵⁹, M. Wu^{114b}, M. Wu¹¹⁶, S.L. Wu¹⁷⁶, S. Wu¹⁴, X. Wu⁶², Y. Wu⁶², Z. Wu⁴, J. Wuerzinger¹¹², T.R. Wyatt¹⁰³, B.M. Wynne⁵², S. Xella⁴³, L. Xia^{114a}, M. Xia¹⁵, M. Xie⁶², A. Xiong¹²⁶, J. Xiong^{18a}, D. Xu¹⁴, H. Xu⁶², L. Xu⁶², R. Xu¹³¹, T. Xu¹⁰⁸, Y. Xu¹⁴², Z. Xu⁵², R. Xue¹³², B. Yabsley¹⁵³, S. Yacoub^{34a}, Y. Yamaguchi⁸⁴, E. Yamashita¹⁵⁹, H. Yamauchi¹⁶³, T. Yamazaki^{18a}, Y. Yamazaki⁸⁶, S. Yan⁵⁹, Z. Yan¹⁰⁵, H.J. Yang^{144a,144b}, H.T. Yang⁶², S. Yang⁶², T. Yang^{64c}, X. Yang³⁷, X. Yang¹⁴, Y. Yang¹⁵⁹, Y. Yang⁶², W-M. Yao^{18a}, C.L. Yardley¹⁵², J. Ye¹⁴, S. Ye³⁰, X. Ye⁶², Y. Yeh⁹⁸, I. Yeletsikh³⁹, B. Yeo^{18b}, M.R. Yexley⁹⁸, T.P. Yildirim¹²⁹, K. Yorita¹⁷⁴, C.J.S. Young³⁷, C. Young¹⁴⁹, N.D. Young¹²⁶, Y. Yu⁶², J. Yuan^{14,114c}, M. Yuan¹⁰⁸, R. Yuan^{144b,144a}, L. Yue⁹⁸, M. Zaazoua⁶², B. Zabinski⁸⁸, I. Zahir^{36a}, A. Zaid^{57b,57a}, Z.K. Zak⁸⁸, T. Zakareishvili¹⁶⁹, S. Zambito⁵⁶, J.A. Zamora Saa^{140d}, J. Zang¹⁵⁹, R. Zanzottera^{71a,71b}, O. Zaplatilek¹³⁵, C. Zeitnitz¹⁷⁷, H. Zeng¹⁴, J.C. Zeng¹⁶⁸, D.T. Zenger Jr²⁷, O. Zenin³⁸, T. Ženiš^{29a}, S. Zenz⁹⁶, D. Zerwas⁶⁶, M. Zhai^{14,114c}, D.F. Zhang¹⁴⁵, G. Zhang¹⁴, J. Zhang^{143a}, J. Zhang⁶, K. Zhang^{14,114c}, L. Zhang⁶², L. Zhang^{114a}, P. Zhang^{14,114c}, R. Zhang^{114a}, S. Zhang⁹¹, T. Zhang¹⁵⁹, Y. Zhang¹⁴², Y. Zhang⁹⁸, Y. Zhang⁶², Y. Zhang^{114a}, Z. Zhang^{143a}, Z. Zhang⁶⁶, H. Zhao¹⁴², T. Zhao^{143a}, Y. Zhao³⁵, Z. Zhao⁶², Z. Zhao⁶², A. Zhemchugov³⁹, J. Zheng^{114a}, K. Zheng¹⁶⁸, X. Zheng⁶², Z. Zheng¹⁴⁹, D. Zhong¹⁶⁸, B. Zhou¹⁰⁸, H. Zhou⁷, N. Zhou^{144a}, Y. Zhou¹⁵, Y. Zhou^{144a}, Y. Zhou⁷, C.G. Zhu^{143a}, J. Zhu¹⁰⁸, X. Zhu^{144b}, Y. Zhu^{144a}, Y. Zhu⁶², X. Zhuang¹⁴, K. Zhukov⁶⁸, N.I. Zimine³⁹, J. Zinsser^{63b}, M. Ziolkowski¹⁴⁷, L. Živković¹⁶, A. Zoccoli^{24b,24a}, K. Zoch⁶¹, A. Zografos³⁷, T.G. Zorbas¹⁴⁵, O. Zormpa⁴⁶, W. Zou⁴², L. Zwalinski³⁷.

¹Department of Physics, University of Adelaide, Adelaide, Australia.

²Department of Physics, University of Alberta, Edmonton AB, Canada.

^{3(a)}Department of Physics, Ankara University, Ankara; ^(b)Division of Physics, TOBB University of Economics and Technology, Ankara, Türkiye.

⁴LAPP, Université Savoie Mont Blanc, CNRS/IN2P3, Annecy, France.

⁵APC, Université Paris Cité, CNRS/IN2P3, Paris, France.

⁶High Energy Physics Division, Argonne National Laboratory, Argonne IL, United States of America.

⁷Department of Physics, University of Arizona, Tucson AZ, United States of America.

⁸Department of Physics, University of Texas at Arlington, Arlington TX, United States of America.

⁹Physics Department, National and Kapodistrian University of Athens, Athens, Greece.

¹⁰Physics Department, National Technical University of Athens, Zografou, Greece.

¹¹Department of Physics, University of Texas at Austin, Austin TX, United States of America.

¹²Institute of Physics, Azerbaijan Academy of Sciences, Baku, Azerbaijan.

¹³Institut de Física d'Altes Energies (IFAE), Barcelona Institute of Science and Technology, Barcelona, Spain.

¹⁴Institute of High Energy Physics, Chinese Academy of Sciences, Beijing, China.

¹⁵Physics Department, Tsinghua University, Beijing, China.

¹⁶Institute of Physics, University of Belgrade, Belgrade, Serbia.

¹⁷Department for Physics and Technology, University of Bergen, Bergen, Norway.

^{18(a)}Physics Division, Lawrence Berkeley National Laboratory, Berkeley CA; ^(b)University of California, Berkeley CA, United States of America.

¹⁹Institut für Physik, Humboldt Universität zu Berlin, Berlin, Germany.

²⁰Albert Einstein Center for Fundamental Physics and Laboratory for High Energy Physics, University of Bern, Bern, Switzerland.

²¹School of Physics and Astronomy, University of Birmingham, Birmingham, United Kingdom.

^{22(a)}Department of Physics, Bogazici University, Istanbul; ^(b)Department of Physics Engineering, Gaziantep University, Gaziantep; ^(c)Department of Physics, Istanbul University, Istanbul, Türkiye.

^{23(a)}Facultad de Ciencias y Centro de Investigaciones, Universidad Antonio Nariño, Bogotá; ^(b)Departamento de Física, Universidad Nacional de Colombia, Bogotá, Colombia.

^{24(a)}Dipartimento di Fisica e Astronomia A. Righi, Università di Bologna, Bologna; ^(b)INFN Sezione di Bologna, Italy.

²⁵Physikalisches Institut, Universität Bonn, Bonn, Germany.

²⁶Department of Physics, Boston University, Boston MA, United States of America.

²⁷Department of Physics, Brandeis University, Waltham MA, United States of America.

^{28(a)}Transilvania University of Brasov, Brasov; ^(b)Horia Hulubei National Institute of Physics and Nuclear Engineering, Bucharest; ^(c)Department of Physics, Alexandru Ioan Cuza University of Iasi, Iasi; ^(d)National Institute for Research and Development of Isotopic and Molecular Technologies, Physics Department, Cluj-Napoca; ^(e)National University of Science and Technology Politehnica, Bucharest; ^(f)West University in Timisoara, Timisoara; ^(g)Faculty of Physics, University of Bucharest, Bucharest, Romania.

^{29(a)}Faculty of Mathematics, Physics and Informatics, Comenius University, Bratislava; ^(b)Department of Subnuclear Physics, Institute of Experimental Physics of the Slovak Academy of Sciences, Kosice, Slovak Republic.

³⁰Physics Department, Brookhaven National Laboratory, Upton NY, United States of America.

³¹Universidad de Buenos Aires, Facultad de Ciencias Exactas y Naturales, Departamento de Física, y CONICET, Instituto de Física de Buenos Aires (IFIBA), Buenos Aires, Argentina.

³²California State University, CA, United States of America.

³³Cavendish Laboratory, University of Cambridge, Cambridge, United Kingdom.

^{34(a)}Department of Physics, University of Cape Town, Cape Town; ^(b)iThemba Labs, Western Cape; ^(c)Department of Mechanical Engineering Science, University of Johannesburg, Johannesburg; ^(d)National Institute of Physics, University of the Philippines Diliman (Philippines); ^(e)Department of Physics, Stellenbosch University, Matieland; ^(f)University of South Africa, Department of Physics, Pretoria; ^(g)University of Zululand, KwaDlangezwa; ^(h)School of Physics, University of the Witwatersrand, Johannesburg, South Africa.

³⁵Department of Physics, Carleton University, Ottawa ON, Canada.

^{36(a)}Faculté des Sciences Ain Chock, Université Hassan II de Casablanca; ^(b)Faculté des Sciences, Université Ibn-Tofail, Kénitra; ^(c)Faculté des Sciences Semlalia, Université Cadi Ayyad, LPHEA-Marrakech; ^(d)LPMR, Faculté des Sciences, Université Mohamed Premier, Oujda; ^(e)Faculté des sciences, Université Mohammed V, Rabat; ^(f)Institute of Applied Physics, Mohammed VI Polytechnic University, Ben Guerir, Morocco.

³⁷CERN, Geneva, Switzerland.

- ³⁸Affiliated with an institute formerly covered by a cooperation agreement with CERN.
- ³⁹Affiliated with an international laboratory covered by a cooperation agreement with CERN.
- ⁴⁰Enrico Fermi Institute, University of Chicago, Chicago IL, United States of America.
- ⁴¹LPC, Université Clermont Auvergne, CNRS/IN2P3, Clermont-Ferrand, France.
- ⁴²Nevis Laboratory, Columbia University, Irvington NY, United States of America.
- ⁴³Niels Bohr Institute, University of Copenhagen, Copenhagen, Denmark.
- ^{44(a)}Dipartimento di Fisica, Università della Calabria, Rende;^(b)INFN Gruppo Collegato di Cosenza, Laboratori Nazionali di Frascati, Italy.
- ⁴⁵Physics Department, Southern Methodist University, Dallas TX, United States of America.
- ⁴⁶National Centre for Scientific Research "Demokritos", Agia Paraskevi, Greece.
- ^{47(a)}Department of Physics, Stockholm University;^(b)Oskar Klein Centre, Stockholm, Sweden.
- ⁴⁸Deutsches Elektronen-Synchrotron DESY, Hamburg and Zeuthen, Germany.
- ⁴⁹Fakultät Physik, Technische Universität Dortmund, Dortmund, Germany.
- ⁵⁰Institut für Kern- und Teilchenphysik, Technische Universität Dresden, Dresden, Germany.
- ⁵¹Department of Physics, Duke University, Durham NC, United States of America.
- ⁵²SUPA - School of Physics and Astronomy, University of Edinburgh, Edinburgh, United Kingdom.
- ⁵³INFN e Laboratori Nazionali di Frascati, Frascati, Italy.
- ⁵⁴Physikalisches Institut, Albert-Ludwigs-Universität Freiburg, Freiburg, Germany.
- ⁵⁵II. Physikalisches Institut, Georg-August-Universität Göttingen, Göttingen, Germany.
- ⁵⁶Département de Physique Nucléaire et Corpusculaire, Université de Genève, Genève, Switzerland.
- ^{57(a)}Dipartimento di Fisica, Università di Genova, Genova;^(b)INFN Sezione di Genova, Italy.
- ⁵⁸II. Physikalisches Institut, Justus-Liebig-Universität Giessen, Giessen, Germany.
- ⁵⁹SUPA - School of Physics and Astronomy, University of Glasgow, Glasgow, United Kingdom.
- ⁶⁰LPSC, Université Grenoble Alpes, CNRS/IN2P3, Grenoble INP, Grenoble, France.
- ⁶¹Laboratory for Particle Physics and Cosmology, Harvard University, Cambridge MA, United States of America.
- ⁶²Department of Modern Physics and State Key Laboratory of Particle Detection and Electronics, University of Science and Technology of China, Hefei, China.
- ^{63(a)}Kirchhoff-Institut für Physik, Ruprecht-Karls-Universität Heidelberg, Heidelberg;^(b)Physikalisches Institut, Ruprecht-Karls-Universität Heidelberg, Heidelberg, Germany.
- ^{64(a)}Department of Physics, Chinese University of Hong Kong, Shatin, N.T., Hong Kong;^(b)Department of Physics, University of Hong Kong, Hong Kong;^(c)Department of Physics and Institute for Advanced Study, Hong Kong University of Science and Technology, Clear Water Bay, Kowloon, Hong Kong, China.
- ⁶⁵Department of Physics, National Tsing Hua University, Hsinchu, Taiwan.
- ⁶⁶IJCLab, Université Paris-Saclay, CNRS/IN2P3, 91405, Orsay, France.
- ⁶⁷Centro Nacional de Microelectrónica (IMB-CNM-CSIC), Barcelona, Spain.
- ⁶⁸Department of Physics, Indiana University, Bloomington IN, United States of America.
- ^{69(a)}INFN Gruppo Collegato di Udine, Sezione di Trieste, Udine;^(b)ICTP, Trieste;^(c)Dipartimento Politecnico di Ingegneria e Architettura, Università di Udine, Udine, Italy.
- ^{70(a)}INFN Sezione di Lecce;^(b)Dipartimento di Matematica e Fisica, Università del Salento, Lecce, Italy.
- ^{71(a)}INFN Sezione di Milano;^(b)Dipartimento di Fisica, Università di Milano, Milano, Italy.
- ^{72(a)}INFN Sezione di Napoli;^(b)Dipartimento di Fisica, Università di Napoli, Napoli, Italy.
- ^{73(a)}INFN Sezione di Pavia;^(b)Dipartimento di Fisica, Università di Pavia, Pavia, Italy.
- ^{74(a)}INFN Sezione di Pisa;^(b)Dipartimento di Fisica E. Fermi, Università di Pisa, Pisa, Italy.
- ^{75(a)}INFN Sezione di Roma;^(b)Dipartimento di Fisica, Sapienza Università di Roma, Roma, Italy.
- ^{76(a)}INFN Sezione di Roma Tor Vergata;^(b)Dipartimento di Fisica, Università di Roma Tor Vergata, Roma, Italy.
- ^{77(a)}INFN Sezione di Roma Tre;^(b)Dipartimento di Matematica e Fisica, Università Roma Tre, Roma, Italy.
- ^{78(a)}INFN-TIFPA;^(b)Università degli Studi di Trento, Trento, Italy.
- ⁷⁹Universität Innsbruck, Department of Astro and Particle Physics, Innsbruck, Austria.
- ⁸⁰University of Iowa, Iowa City IA, United States of America.
- ⁸¹Department of Physics and Astronomy, Iowa State University, Ames IA, United States of America.
- ⁸²Istinye University, Sariyer, Istanbul, Türkiye.
- ^{83(a)}Departamento de Engenharia Elétrica, Universidade Federal de Juiz de Fora (UFJF), Juiz de Fora;^(b)Universidade Federal do Rio De Janeiro COPPE/EE/IF, Rio de Janeiro;^(c)Instituto de Física, Universidade de São Paulo, São Paulo;^(d)Rio de Janeiro State University, Rio de Janeiro;^(e)Federal University of Bahia, Bahia, Brazil.
- ⁸⁴KEK, High Energy Accelerator Research Organization, Tsukuba, Japan.
- ^{85(a)}Khalifa University of Science and Technology, Abu Dhabi;^(b)University of Sharjah, Sharjah, United Arab Emirates.
- ⁸⁶Graduate School of Science, Kobe University, Kobe, Japan.
- ^{87(a)}AGH University of Krakow, Faculty of Physics and Applied Computer Science, Krakow;^(b)Marian Smoluchowski Institute of Physics, Jagiellonian University, Krakow, Poland.
- ⁸⁸Institute of Nuclear Physics Polish Academy of Sciences, Krakow, Poland.
- ⁸⁹Faculty of Science, Kyoto University, Kyoto, Japan.
- ⁹⁰Research Center for Advanced Particle Physics and Department of Physics, Kyushu University, Fukuoka, Japan.
- ⁹¹L2IT, Université de Toulouse, CNRS/IN2P3, UPS, Toulouse, France.
- ⁹²Instituto de Física La Plata, Universidad Nacional de La Plata and CONICET, La Plata, Argentina.
- ⁹³Physics Department, Lancaster University, Lancaster, United Kingdom.
- ⁹⁴Oliver Lodge Laboratory, University of Liverpool, Liverpool, United Kingdom.
- ⁹⁵Department of Experimental Particle Physics, Jožef Stefan Institute and Department of Physics, University of Ljubljana, Ljubljana, Slovenia.
- ⁹⁶Department of Physics and Astronomy, Queen Mary University of London, London, United Kingdom.
- ⁹⁷Department of Physics, Royal Holloway University of London, Egham, United Kingdom.
- ⁹⁸Department of Physics and Astronomy, University College London, London, United Kingdom.
- ⁹⁹Louisiana Tech University, Ruston LA, United States of America.
- ¹⁰⁰Fysiska institutionen, Lunds universitet, Lund, Sweden.
- ¹⁰¹Departamento de Física Teórica C-15 and CIAFF, Universidad Autónoma de Madrid, Madrid, Spain.
- ¹⁰²Institut für Physik, Universität Mainz, Mainz, Germany.
- ¹⁰³School of Physics and Astronomy, University of Manchester, Manchester, United Kingdom.

- ¹⁰⁴CPPM, Aix-Marseille Université, CNRS/IN2P3, Marseille, France.
- ¹⁰⁵Department of Physics, University of Massachusetts, Amherst MA, United States of America.
- ¹⁰⁶Department of Physics, McGill University, Montreal QC, Canada.
- ¹⁰⁷School of Physics, University of Melbourne, Victoria, Australia.
- ¹⁰⁸Department of Physics, University of Michigan, Ann Arbor MI, United States of America.
- ¹⁰⁹Department of Physics and Astronomy, Michigan State University, East Lansing MI, United States of America.
- ¹¹⁰Group of Particle Physics, University of Montreal, Montreal QC, Canada.
- ¹¹¹Fakultät für Physik, Ludwig-Maximilians-Universität München, München, Germany.
- ¹¹²Max-Planck-Institut für Physik (Werner-Heisenberg-Institut), München, Germany.
- ¹¹³Graduate School of Science and Kobayashi-Maskawa Institute, Nagoya University, Nagoya, Japan.
- ¹¹⁴(^a)Department of Physics, Nanjing University, Nanjing; (^b)School of Science, Shenzhen Campus of Sun Yat-sen University; (^c)University of Chinese Academy of Science (UCAS), Beijing, China.
- ¹¹⁵Department of Physics and Astronomy, University of New Mexico, Albuquerque NM, United States of America.
- ¹¹⁶Institute for Mathematics, Astrophysics and Particle Physics, Radboud University/Nikhef, Nijmegen; Netherlands.
- ¹¹⁷Nikhef National Institute for Subatomic Physics and University of Amsterdam, Amsterdam, Netherlands.
- ¹¹⁸Department of Physics, Northern Illinois University, DeKalb IL, United States of America.
- ¹¹⁹(^a)New York University Abu Dhabi, Abu Dhabi; (^b)United Arab Emirates University, Al Ain, United Arab Emirates.
- ¹²⁰Department of Physics, New York University, New York NY, United States of America.
- ¹²¹Ochanomizu University, Otsuka, Bunkyo-ku, Tokyo, Japan.
- ¹²²Ohio State University, Columbus OH, United States of America.
- ¹²³Homer L. Dodge Department of Physics and Astronomy, University of Oklahoma, Norman OK, United States of America.
- ¹²⁴Department of Physics, Oklahoma State University, Stillwater OK, United States of America.
- ¹²⁵Palacký University, Joint Laboratory of Optics, Olomouc, Czech Republic.
- ¹²⁶Institute for Fundamental Science, University of Oregon, Eugene, OR, United States of America.
- ¹²⁷Graduate School of Science, University of Osaka, Osaka, Japan.
- ¹²⁸Department of Physics, University of Oslo, Oslo, Norway.
- ¹²⁹Department of Physics, Oxford University, Oxford, United Kingdom.
- ¹³⁰LPNHE, Sorbonne Université, Université Paris Cité, CNRS/IN2P3, Paris, France.
- ¹³¹Department of Physics, University of Pennsylvania, Philadelphia PA, United States of America.
- ¹³²Department of Physics and Astronomy, University of Pittsburgh, Pittsburgh PA, United States of America.
- ¹³³(^a)Laboratório de Instrumentação e Física Experimental de Partículas - LIP, Lisboa; (^b)Departamento de Física, Faculdade de Ciências, Universidade de Lisboa, Lisboa; (^c)Departamento de Física, Universidade de Coimbra, Coimbra; (^d)Centro de Física Nuclear da Universidade de Lisboa, Lisboa; (^e)Departamento de Física, Escola de Ciências, Universidade do Minho, Braga; (^f)Departamento de Física Teórica y del Cosmos, Universidad de Granada, Granada (Spain); (^g)Departamento de Física, Instituto Superior Técnico, Universidade de Lisboa, Lisboa, Portugal.
- ¹³⁴Institute of Physics of the Czech Academy of Sciences, Prague, Czech Republic.
- ¹³⁵Czech Technical University in Prague, Prague, Czech Republic.
- ¹³⁶Charles University, Faculty of Mathematics and Physics, Prague, Czech Republic.
- ¹³⁷Particle Physics Department, Rutherford Appleton Laboratory, Didcot, United Kingdom.
- ¹³⁸IRFU, CEA, Université Paris-Saclay, Gif-sur-Yvette, France.
- ¹³⁹Santa Cruz Institute for Particle Physics, University of California Santa Cruz, Santa Cruz CA, United States of America.
- ¹⁴⁰(^a)Departamento de Física, Pontificia Universidad Católica de Chile, Santiago; (^b)Millennium Institute for Subatomic physics at high energy frontier (SAPHIR), Santiago; (^c)Instituto de Investigación Multidisciplinario en Ciencia y Tecnología, y Departamento de Física, Universidad de La Serena; (^d)Universidad Andres Bello, Department of Physics, Santiago; (^e)Universidad San Sebastian, Recoleta; (^f)Instituto de Alta Investigación, Universidad de Tarapacá, Arica; (^g)Departamento de Física, Universidad Técnica Federico Santa María, Valparaíso, Chile.
- ¹⁴¹Department of Physics, Institute of Science, Tokyo, Japan.
- ¹⁴²Department of Physics, University of Washington, Seattle WA, United States of America.
- ¹⁴³(^a)Institute of Frontier and Interdisciplinary Science and Key Laboratory of Particle Physics and Particle Irradiation (MOE), Shandong University, Qingdao (^b)School of Physics, Zhengzhou University, China.
- ¹⁴⁴(^a)State Key Laboratory of Dark Matter Physics, School of Physics and Astronomy, Shanghai Jiao Tong University, Key Laboratory for Particle Astrophysics and Cosmology (MOE), SKLPPC, Shanghai; (^b)State Key Laboratory of Dark Matter Physics, Tsung-Dao Lee Institute, Shanghai Jiao Tong University, Shanghai, China.
- ¹⁴⁵Department of Physics and Astronomy, University of Sheffield, Sheffield, United Kingdom.
- ¹⁴⁶Department of Physics, Shinshu University, Nagano, Japan.
- ¹⁴⁷Department Physik, Universität Siegen, Siegen, Germany.
- ¹⁴⁸Department of Physics, Simon Fraser University, Burnaby BC, Canada.
- ¹⁴⁹SLAC National Accelerator Laboratory, Stanford CA, United States of America.
- ¹⁵⁰Department of Physics, Royal Institute of Technology, Stockholm, Sweden.
- ¹⁵¹Departments of Physics and Astronomy, Stony Brook University, Stony Brook NY, United States of America.
- ¹⁵²Department of Physics and Astronomy, University of Sussex, Brighton, United Kingdom.
- ¹⁵³School of Physics, University of Sydney, Sydney, Australia.
- ¹⁵⁴Institute of Physics, Academia Sinica, Taipei, Taiwan.
- ¹⁵⁵(^a)E. Andronikashvili Institute of Physics, Iv. Javakishvili Tbilisi State University, Tbilisi; (^b)High Energy Physics Institute, Tbilisi State University, Tbilisi; (^c)University of Georgia, Tbilisi, Georgia.
- ¹⁵⁶Department of Physics, Technion, Israel Institute of Technology, Haifa, Israel.
- ¹⁵⁷Raymond and Beverly Sackler School of Physics and Astronomy, Tel Aviv University, Tel Aviv, Israel.
- ¹⁵⁸Department of Physics, Aristotle University of Thessaloniki, Thessaloniki, Greece.
- ¹⁵⁹International Center for Elementary Particle Physics and Department of Physics, University of Tokyo, Tokyo, Japan.
- ¹⁶⁰Graduate School of Science and Technology, Tokyo Metropolitan University, Tokyo, Japan.
- ¹⁶¹Department of Physics, University of Toronto, Toronto ON, Canada.
- ¹⁶²(^a)TRIUMF, Vancouver BC; (^b)Department of Physics and Astronomy, York University, Toronto ON, Canada.
- ¹⁶³Division of Physics and Tomonaga Center for the History of the Universe, Faculty of Pure and Applied Sciences, University of Tsukuba, Tsukuba, Japan.
- ¹⁶⁴Department of Physics and Astronomy, Tufts University, Medford MA, United States of America.
- ¹⁶⁵Department of Physics and Astronomy, University of California Irvine, Irvine CA, United States of America.
- ¹⁶⁶University of West Attica, Athens, Greece.
- ¹⁶⁷Department of Physics and Astronomy, University of Uppsala, Uppsala, Sweden.

¹⁶⁸Department of Physics, University of Illinois, Urbana IL, United States of America.

¹⁶⁹Instituto de Física Corpuscular (IFIC), Centro Mixto Universidad de Valencia - CSIC, Valencia, Spain.

¹⁷⁰Department of Physics, University of British Columbia, Vancouver BC, Canada.

¹⁷¹Department of Physics and Astronomy, University of Victoria, Victoria BC, Canada.

¹⁷²Fakultät für Physik und Astronomie, Julius-Maximilians-Universität Würzburg, Würzburg, Germany.

¹⁷³Department of Physics, University of Warwick, Coventry, United Kingdom.

¹⁷⁴Waseda University, Tokyo, Japan.

¹⁷⁵Department of Particle Physics and Astrophysics, Weizmann Institute of Science, Rehovot, Israel.

¹⁷⁶Department of Physics, University of Wisconsin, Madison WI, United States of America.

¹⁷⁷Fakultät für Mathematik und Naturwissenschaften, Fachgruppe Physik, Bergische Universität Wuppertal, Wuppertal, Germany.

¹⁷⁸Department of Physics, Yale University, New Haven CT, United States of America.

¹⁷⁹Yerevan Physics Institute, Yerevan, Armenia.

^aAlso at Affiliated with an institute formerly covered by a cooperation agreement with CERN.

^bAlso at An-Najah National University, Nablus, Palestine.

^cAlso at Borough of Manhattan Community College, City University of New York, New York NY, United States of America.

^dAlso at Center for Interdisciplinary Research and Innovation (CIRI-AUTH), Thessaloniki, Greece.

^eAlso at Centre of Physics of the Universities of Minho and Porto (CF-UM-UP), Portugal.

^fAlso at CERN, Geneva, Switzerland.

^gAlso at CMD-AC UNEC Research Center, Azerbaijan State University of Economics (UNEC), Azerbaijan.

^hAlso at Département de Physique Nucléaire et Corpusculaire, Université de Genève, Genève, Switzerland.

ⁱAlso at Departament de Física de la Universitat Autònoma de Barcelona, Barcelona, Spain.

^jAlso at Department of Financial and Management Engineering, University of the Aegean, Chios, Greece.

^kAlso at Department of Mathematical Sciences, University of South Africa, Johannesburg, South Africa.

^lAlso at Department of Modern Physics and State Key Laboratory of Particle Detection and Electronics, University of Science and Technology of China, Hefei, China.

^mAlso at Department of Physics, Bolu Abant İzzet Baysal University, Bolu, Türkiye.

ⁿAlso at Department of Physics, King's College London, London, United Kingdom.

^oAlso at Department of Physics, Stanford University, Stanford CA, United States of America.

^pAlso at Department of Physics, Stellenbosch University, South Africa.

^qAlso at Department of Physics, University of Fribourg, Fribourg, Switzerland.

^rAlso at Department of Physics, University of Thessaly, Greece.

^sAlso at Department of Physics, Westmont College, Santa Barbara, United States of America.

^tAlso at Faculty of Physics, Sofia University, 'St. Kliment Ohridski', Sofia, Bulgaria.

^uAlso at Faculty of Physics, University of Bucharest, Romania.

^vAlso at Hellenic Open University, Patras, Greece.

^wAlso at Henan University, China.

^xAlso at Imam Mohammad Ibn Saud Islamic University, Saudi Arabia.

^yAlso at Institutio Catalana de Recerca i Estudis Avançats, ICREA, Barcelona, Spain.

^zAlso at Institut für Experimentalphysik, Universität Hamburg, Hamburg, Germany.

^{aa}Also at Institute for Nuclear Research and Nuclear Energy (INRNE) of the Bulgarian Academy of Sciences, Sofia, Bulgaria.

^{ab}Also at Institute of Applied Physics, Mohammed VI Polytechnic University, Ben Guerir, Morocco.

^{ac}Also at Institute of Particle Physics (IPP), Canada.

^{ad}Also at Institute of Physics and Technology, Mongolian Academy of Sciences, Ulaanbaatar, Mongolia.

^{ae}Also at Institute of Physics, Azerbaijan Academy of Sciences, Baku, Azerbaijan.

^{af}Also at Institute of Theoretical Physics, Ilia State University, Tbilisi, Georgia.

^{ag}Also at National Institute of Physics, University of the Philippines Diliman (Philippines), Philippines.

^{ah}Also at The Collaborative Innovation Center of Quantum Matter (CI-CQM), Beijing, China.

^{ai}Also at TRIUMF, Vancouver BC, Canada.

^{aj}Also at Università di Napoli Parthenope, Napoli, Italy.

^{ak}Also at University of Colorado Boulder, Department of Physics, Colorado, United States of America.

^{al}Also at University of Sienna, Italy.

^{am}Also at Washington College, Chestertown, MD, United States of America.

^{an}Also at Yeditepe University, Physics Department, Istanbul, Türkiye.

*Deceased

References

- [1] L. Evans, P. Bryant, LHC Machine, JINST 3 (2008) S08001. <https://doi.org/10.1088/1748-0221/3/08/S08001>
- [2] W. Busza, K. Rajagopal, W. van der Schee, Heavy ion collisions: the big picture, and the big questions, Ann. Rev. Nucl. Part. Sci. 68 (2018) 339–376. <https://doi.org/10.1146/annurev-nucl-101917-020852>
- [3] E. Shuryak, Strongly coupled quark-gluon plasma in heavy ion collisions, Rev. Mod. Phys. 89 (2017) 035001. <https://doi.org/10.1103/RevModPhys.89.035001>
- [4] J. Casalderrey-Solana, C.A. Salgado, Introductory lectures on jet quenching in heavy ion collisions, Acta Phys. Polon. B 38 (2007) 3731–3794. [arXiv preprint arXiv:0712.3443](https://arxiv.org/abs/0712.3443).
- [5] D. d'Enterria, Jet quenching, Landolt-Bornstein 23 (2010) 471. https://doi.org/10.1007/978-3-642-01539-7_16
- [6] U.A. Wiedemann, Jet quenching in heavy ion collisions, Landolt-Bornstein (2010) 521–562. https://doi.org/10.1007/978-3-642-01539-7_17
- [7] A. Majumder, M. Van Leeuwen, The theory and phenomenology of perturbative QCD based jet quenching, Prog. Part. Nucl. Phys. 66 (2011) 41–92. <https://doi.org/10.1016/j.pnpnp.2010.09.001>
- [8] Y. Mehtar-Tani, J.G. Milhano, K. Tywoniuk, Jet physics in heavy-ion collisions, Int. J. Mod. Phys. A 28 (2013) 1340013. <https://doi.org/10.1142/S0217751X13400137>
- [9] S. Cao, X.-N. Wang, Jet quenching and medium response in high-energy heavy-ion collisions: a review, Rept. Prog. Phys. 84 (2) (2021) 024301. <https://doi.org/10.1088/1361-6633/abc22b>
- [10] M. Connors, C. Nattrass, R. Reed, S. Salur, Jet measurements in heavy ion physics, Rev. Mod. Phys. 90 (2018) 025005. <https://doi.org/10.1103/RevModPhys.90.025005>
- [11] L. Cunqueiro, A.M. Sickles, Studying the QGP with jets at the LHC and RHIC, Prog. Part. Nucl. Phys. 124 (2022) 103940. <https://doi.org/10.1016/j.pnpnp.2022.103940>
- [12] L. Apolinário, Y.-T. Chien, L. Cunqueiro Mendez, Jet substructure, Int. J. Mod. Phys. E 33 (07) (2024) 2430003. <https://doi.org/10.1142/S0218301324300030>
- [13] Y. Mehtar-Tani, C.A. Salgado, K. Tywoniuk, Antiangular ordering of gluon radiation in QCD media, Phys. Rev. Lett. 106 (2011) 122002. <https://doi.org/10.1103/PhysRevLett.106.122002>
- [14] Y. Mehtar-Tani, K. Tywoniuk, Jet coherence in QCD media: the antenna radiation spectrum, JHEP 01 (2013) 031. [https://doi.org/10.1007/JHEP01\(2013\)031](https://doi.org/10.1007/JHEP01(2013)031)
- [15] Y. Mehtar-Tani, C.A. Salgado, K. Tywoniuk, Jets in QCD media: from color coherence to decoherence, Phys. Lett. B 707 (2012) 156–159. <https://doi.org/10.1016/j.physletb.2011.12.042>
- [16] J. Casalderrey-Solana, Y. Mehtar-Tani, C.A. Salgado, K. Tywoniuk, New picture of jet quenching dictated by color coherence, Phys. Lett. B 725 (2013) 357–360. <https://doi.org/10.1016/j.physletb.2013.07.046>
- [17] Z. Hulcher, D. Pablos, K. Rajagopal, Resolution effects in the hybrid strong/weak coupling model, JHEP 03 (2018) 010. [https://doi.org/10.1007/JHEP03\(2018\)010](https://doi.org/10.1007/JHEP03(2018)010)
- [18] H.A. Andrews, et al., Novel tools and observables for jet physics in heavy-ion collisions, J. Phys. G 47 (6) (2020) 065102. <https://doi.org/10.1088/1361-6471/ab7c9c>
- [19] CMS Collaboration, Measurement of the Splitting Function in pp and Pb–Pb Collisions at $\sqrt{s_{NN}} = 5.02$ TeV, Phys. Rev. Lett. 120 (2018) 142302. <https://doi.org/10.1103/PhysRevLett.120.142302>
- [20] ALICE Collaboration, A Large Ion Collider Experiment, ALICE, Measurement of the groomed jet radius and momentum splitting fraction in pp and Pb–Pb collisions

- at $\sqrt{s_{NN}} = 5.02$ TeV, Phys. Rev. Lett. 128 (10) (2022) 102001. <https://doi.org/10.1103/PhysRevLett.128.102001>
- [21] CMS Collaboration, Girth and groomed radius of jets recoiling against isolated photons in lead–lead and proton–proton collisions at $\sqrt{s_{NN}} = 5.02$ TeV, Phys. Lett. B 861 (2025) 139088. <https://doi.org/10.1016/j.physletb.2024.139088>
- [22] ATLAS Collaboration, Measurement of substructure-dependent jet suppression in Pb+Pb collisions at 5.02 TeV with the ATLAS detector, Phys. Rev. C 107 (2023) 054909. <https://doi.org/10.1103/PhysRevC.107.054909>
- [23] ALICE Collaboration, ALICE, Exploration of jet substructure using iterative declustering in pp and Pb–Pb collisions at LHC energies, Phys. Lett. B 802 (2020) 135227. <https://doi.org/10.1016/j.physletb.2020.135227>
- [24] ATLAS Collaboration, Measurement of Suppression of Large-Radius Jets and Its Dependence on Substructure in Pb+Pb Collisions at $\sqrt{s_{NN}} = 5.02$ TeV with the ATLAS detector, Phys. Rev. Lett. 131 (2023) 172301. <https://doi.org/10.1103/PhysRevLett.131.172301>
- [25] ALICE Collaboration, ALICE, First measurements of N-subjettiness in central Pb–Pb collisions at $\sqrt{s_{NN}} = 2.76$ TeV, JHEP 10 (2021) 003. [https://doi.org/10.1007/JHEP10\(2021\)003](https://doi.org/10.1007/JHEP10(2021)003)
- [26] ATLAS Collaboration, Measurement of angular and momentum distributions of charged particles within and around jets in Pb+Pb and pp collisions at $\sqrt{s_{NN}} = 5.02$ TeV with the ATLAS detector, Phys. Rev. C 100 (2019) 064901. <https://doi.org/10.1103/PhysRevC.100.064901>
- [27] J.M. Butterworth, A.R. Davison, M. Rubin, G.P. Salam, Jet substructure as a new higgs-Search channel at the large hadron collider, Phys. Rev. Lett. 100 (2008) 242001. <https://doi.org/10.1103/PhysRevLett.100.242001>
- [28] S. Marzani, G. Soyez, M. Spannowsky, Looking inside jets: an introduction to jet substructure and boosted-object phenomenology, Lect. Notes Phys. 958 (2019). <https://doi.org/10.1007/978-3-030-15709-8>
- [29] A.J. Larkoski, S. Marzani, G. Soyez, J. Thaler, Soft drop, JHEP 05 (2014) 146. [https://doi.org/10.1007/JHEP05\(2014\)146](https://doi.org/10.1007/JHEP05(2014)146)
- [30] A.S. Kudinoor, D. Pablos, K. Rajagopal, Visualizing how the structure of large-Radius jets shapes their wakes (2025). [arXiv preprint arXiv:2501.18683](https://arxiv.org/abs/2501.18683)
- [31] J. Casalderruy-Solana, D.C. Gulhan, J.G. Milhano, D. Pablos, K. Rajagopal, A hybrid strong/weak coupling approach to jet quenching, JHEP 10 (2014) 019. [https://doi.org/10.1007/JHEP10\(2014\)019](https://doi.org/10.1007/JHEP10(2014)019)
- [32] ATLAS Collaboration, The ATLAS Experiment at the CERN Large Hadron Collider, JINST 3 (2008) S08003. <https://doi.org/10.1088/1748-0221/3/08/S08003>
- [33] ATLAS Collaboration, Performance of the ATLAS trigger system in 2015, Eur. Phys. J. C 77 (2017) 317. <https://doi.org/10.1140/epjc/s10052-017-4852-3>
- [34] ATLAS Collaboration, Software and computing for run 3 of the ATLAS experiment at the LHC, Eur. Phys. J. C 85 (2025) 234. <https://doi.org/10.1140/epjc/s10052-024-13701-w>
- [35] ATLAS Collaboration, ATLAS Data quality operations and performance for 2015–2018 data-taking, JINST 15 (2020) P04003. <https://doi.org/10.1088/1748-0221/15/04/P04003>
- [36] ATLAS Collaboration, Trigger Menu in 2018, ATL-DAQ-PUB-2019-001, 2019. <https://cds.cern.ch/record/2693402>
- [37] ATLAS Collaboration, Vertex Reconstruction Performance of the ATLAS Detector at $\sqrt{s} = 13$ TeV, ATL-PHYS-PUB-2015-026, 2015. <https://cds.cern.ch/record/2037717>
- [38] M.L. Miller, K. Reygers, S.J. Sanders, P. Steinberg, Glauber modeling in high-energy nuclear collisions, Ann. Rev. Nucl. Part. Sci. 57 (2007) 205–243. <https://doi.org/10.1146/annurev.nucl.57.090506.123020>
- [39] ATLAS Collaboration, Jet radius dependence of dijet momentum balance and suppression in Pb+Pb collisions at 5.02 TeV with the ATLAS detector, Phys. Rev. C 110 (2024) 054912. <https://doi.org/10.1103/PhysRevC.110.054912>
- [40] T. Sjöstrand, S. Ask, J.R. Christiansen, R. Corke, N. Desai, P. Ilten, S. Mrenna, S. Prestel, C.O. Rasmussen, P.Z. Skands, An introduction to PYTHIA 8.2, Comput. Phys. Commun. 191 (2015) 159. <https://doi.org/10.1016/j.cpc.2015.01.024>
- [41] ATLAS Collaboration, ATLAS Pythia 8 tunes to 7 TeV data, ATL-PHYS-PUB-2014-021, 2014. <https://cds.cern.ch/record/1966419>
- [42] NNPDF Collaboration, R.D. Ball, et al., Parton distributions with LHC data, Nucl. Phys. B 867 (2013) 244. <https://doi.org/10.1016/j.nuclphysb.2012.10.003>
- [43] T. Sjöstrand, S. Mrenna, P. Skands, A brief introduction to PYTHIA 8.1, Comput. Phys. Commun. 178 (2008) 852–867. <https://doi.org/10.1016/j.cpc.2008.01.036>
- [44] ATLAS Collaboration, The Pythia 8 A3 tune description of ATLAS minimum bias and inelastic measurements incorporating the Donnachie–Landshoff diffractive model, ATL-PHYS-PUB-2016-017, 2016. <https://cds.cern.ch/record/2206965>
- [45] S. Agostinelli, et al., GEANT4, GEANT4 - a simulation toolkit, Nucl. Instrum. Meth. A 506 (2003) 250–303. [https://doi.org/10.1016/S0168-9002\(03\)01368-8](https://doi.org/10.1016/S0168-9002(03)01368-8)
- [46] ATLAS Collaboration, The ATLAS simulation infrastructure, Eur. Phys. J. C 70 (2010) 823. <https://doi.org/10.1140/epjc/s10052-010-1429-9>
- [47] M. Cacciari, G.P. Salam, G. Soyez, The anti- k_r jet clustering algorithm, JHEP 04 (2008) 063. <https://doi.org/10.1088/1126-6708/2008/04/063>
- [48] M. Cacciari, G.P. Salam, G. Soyez, Fastjet user manual, Eur. Phys. J. C 72 (2012) 1896. <https://doi.org/10.1140/epjc/s10052-012-1896-2>
- [49] ATLAS Collaboration, Measurement of the nuclear modification factor for inclusive jets in Pb+Pb collisions at $\sqrt{s_{NN}} = 5.02$ TeV with the ATLAS detector, Phys. Lett. B 790 (2019) 108. <https://doi.org/10.1016/j.physletb.2018.10.076>
- [50] ATLAS Collaboration, Measurement of the jet radius and transverse momentum dependence of inclusive jet suppression in lead–lead collisions at $\sqrt{s_{NN}} = 2.76$ TeV with the ATLAS detector, Phys. Lett. B 719 (2013) 220. <https://doi.org/10.1016/j.physletb.2013.01.024>
- [51] ATLAS Collaboration, Jet energy scale and resolution measured in proton–proton collisions at $\sqrt{s} = 13$ TeV with the ATLAS detector, Eur. Phys. J. C 81 (2021) 689. <https://doi.org/10.1140/epjc/s10052-021-09402-3>
- [52] ATLAS Collaboration, Jet energy scale and its uncertainty for jets reconstructed using the ATLAS heavy ion jet algorithm, ATLAS-CONF-2015-016, 2015. <https://cds.cern.ch/record/2008677>
- [53] ATLAS Collaboration, Performance of the ATLAS track reconstruction algorithms in dense environments in LHC run 2, Eur. Phys. J. C 77 (2017) 673. <https://doi.org/10.1140/epjc/s10052-017-5225-7>
- [54] M. Cacciari, G.P. Salam, Pileup subtraction using jet areas, Phys. Lett. B 659 (2008) 119–126. <https://doi.org/10.1016/j.physletb.2007.09.077>
- [55] M. Cacciari, G.P. Salam, G. Soyez, The catchment area of jets, JHEP 04 (2008) 005. <https://doi.org/10.1088/1126-6708/2008/04/005>
- [56] S. Catani, Y.L. Dokshitzer, M.H. Seymour, B.R. Webber, Longitudinally-invariant k_T -clustering algorithms for hadron-hadron collisions, Nucl. Phys. B 406 (1993) 187–224. [https://doi.org/10.1016/0550-3213\(93\)90166-M](https://doi.org/10.1016/0550-3213(93)90166-M)
- [57] ATLAS Collaboration, Measurements of the nuclear modification factor for jets in pb+pb collisions at $\sqrt{s_{NN}} = 2.76$ TeV with the ATLAS detector, Phys. Rev. Lett. 114 (2015) 072302. <https://doi.org/10.1103/PhysRevLett.114.072302>
- [58] G. D’Agostini, A multidimensional unfolding method based on Bayes’ theorem, Nucl. Instrum. Meth. A 362 (1995) 487–498. [https://doi.org/10.1016/0168-9002\(95\)00274-X](https://doi.org/10.1016/0168-9002(95)00274-X)
- [59] T. Adye, Unfolding algorithms and tests using RooUnfold, in: Proceedings, 2011 Workshop on Statistical Issues Related to Discovery Claims in Search Experiments and Unfolding (PHYSTAT 2011), pp. 313–318. <https://doi.org/10.5170/CERN-2011-006.313>
- [60] ATLAS Collaboration, Early Inner Detector Tracking Performance in the 2015 Data at $\sqrt{s} = 13$ TeV, ATL-PHYS-PUB-2015-051, 2015. <https://cds.cern.ch/record/2110140>
- [61] ATLAS Collaboration, Measurement of Track Reconstruction Inefficiencies in the Core of Jets Via Pixel dE/dx With the ATLAS Experiment Using $\sqrt{s} = 13$ TeV pp Collision Data, ATL-PHYS-PUB-2016-007, 2016. <https://cds.cern.ch/record/2140460>
- [62] ATLAS Collaboration, Luminosity determination in pp collisions at $\sqrt{s} = 13$ TeV using the ATLAS detector at the LHC, Eur. Phys. J. C 83 (2023) 982. <https://doi.org/10.1140/epjc/s10052-023-11747-w>
- [63] G. Avoni, et al., The new LUCID-2 detector for luminosity measurement and monitoring in ATLAS, JINST 13 (2018) P07017. <https://doi.org/10.1088/1748-0221/13/07/P07017>
- [64] ATLAS Collaboration, ATLAS Computing Acknowledgements, ATL-SOFT-PUB-2025-001, 2025. <https://cds.cern.ch/record/2922210>
- [65] ATLAS Collaboration, CERN, CERN Open Data Policy for the LHC Experiments, CERN-OPEN-2020-013, (2020). <https://cds.cern.ch/record/2745133>